NIST Technical Note
NIST TN 2379

Determination of Per- and Polyfluoroalkyl Substances and Other Halogenated Compounds using Combustion Ion Chromatography

Halen D. Solomon
Andrew C. Maizel
Audrey F. Tombaugh
Brittany L. Stinger
Andre L. Thompson
Rick D. Davis

This publication is available free of charge from:
https://doi.org/10.6028/NIST.TN.2379

NIST NATIONAL INSTITUTE OF STANDARDS AND TECHNOLOGY
U.S. DEPARTMENT OF COMMERCE

NIST Technical Note
NIST TN 2379

Determination of Per- and Polyfluoroalkyl Substances and Other Halogenated Compounds using Combustion Ion Chromatography

Halen D. Solomon*
Fire Research Division
Engineering Laboratory
Department of Chemical and Environmental Engineering
Yale University

Andrew C. Maizel*
Audrey F. Tombaugh
Brittany L. Stinger
Andre L. Thompson
Rick D. Davis
Fire Research Division
Engineering Laboratory

**Former NIST employee; all work for this publication was done while at NIST*

This publication is available free of charge from:
https://doi.org/10.6028/NIST.TN.2379

July 2026

U.S. Department of Commerce
Howard Lutnick, Secretary

National Institute of Standards and Technology
Arvind Raman, NIST Director and Under Secretary of Commerce for Standards and Technology

NIST TN 2379
July 2026

Publication History
Approved by the NIST Editorial Review Board on 2026-07-21

How to Cite this NIST Technical Series Publication
Solomon HD; Maizel AC; Tombaugh AF; Stinger BL; Andre L. Thompson AL; Davis RD. (2026) Determination of Per- and Polyfluoroalkyl Substances and Other Halogenated Compounds using Combustion Ion Chromatography. (National Institute of Standards and Technology, Gaithersburg, MD), NIST Technical Note (TN) NIST TN 2379. https://doi.org/10.6028/NIST.TN.2379

Author ORCID iDs
Halen D. Solomon: 0000-0002-8664-9577
Andrew C. Maizel: 0000-0002-2981-5241
Audrey F. Tombaugh: 0009-0008-4656-2742
Brittany L. Stinger: 0009-0000-7231-8307
Andre L. Thompson: 0000-0001-5717-6902
Rick. D. Davis: 0000-0003-2264-0490

Contact Information
rick.davis@nist.gov

Abstract

This NIST Technical Note describes the use of combustion ion chromatography to measure halogen content (fluorine, chlorine, and bromine) in a variety of solid and liquid matrices, with a particular focus on materials containing per- and polyfluoroalkyl substances (PFAS). The research examines the major contributors to measurement uncertainty, including sample combustion mass, calibration curve development, background contamination, matrix effects, and instrument response. Method performance was improved through instrument calibration, blank subtraction and approaches to account for matrix-dependent behavior. The use of a partial loop injection system was also evaluated as an approach to extend the effective measurement range, including its impact on uncertainties. The effects of cations, variabilities in fluoride sensitivity, and incomplete PFAS combustion were studied using NIST SRM 2143, 3181, 3182, 3183, 3184, 3186, NIST RM 8446, and additional 3rd-party reference standards. Concurrent determination of sulfur was also determined. This Technical Note provides new combustion efficiency and fluorine recovery values for selected NIST SRMs and RMs, along with several fluorotelomer alcohol and fluorotelomer acrylate compounds.

Keywords

Combustion ion chromatography; CIC; fluorine; chlorine; halogens; lithium; per- and polyfluoroalkyl substances; PFAS

Table of Contents

1. Introduction 1
2. Materials and Methods 3
2.1. Consumables Preparation and Instrument Setup 3
2.1.1. Illustrative Guide 5
2.2. Reference Materials and Analytical Standards 8
2.3. Analytical Run Setup 13
2.4. Instrument Response and the Characterization of Partial Loop Injection System 15
2.5. Blank Subtraction and Determination of Halogen Mass Fractions 17
2.5.1. Determination of Halogen Mass Fractions 17
2.5.1.1. Concentration and Mass Fraction Using Direct Injection 17
2.5.1.2. Mass Fraction Using Combustion Ion Chromatography 17
2.5.1.3. Blank Subtraction 17
2.5.1.4. Limit of Determination and Limit of Quantitation 18
2.6. Organofluorine and Organochlorine Calibration Curve Creation using NIST RM 8446, NIST SRM 2143 and 2144 19
2.7. Fluorine Recovery of PFAS and Other Organofluorines 21
2.8. Effects of Cations on Fluoride Measurements 21
2.9. Concurrent Sulfur Determinations 21
3. Measurement Uncertainties 22
3.1. Volumetric Measurements 22
3.1.1. 2 mL Motorized Burettes 23
3.1.2. 5 mL Motorized Burettes 23
3.1.3. 10 mL Motorized Burettes 23
3.1.4. Estimated Uncertainties for IC Injection Volumes 23
3.2. Conductivity Measurements and Peak Area Integrations 24
3.3. Mass and Mass Fraction Measurements 25
3.3.1. Masses Weighed to 5 Decimal Points 25
3.3.2. Masses Weighed to 2 Decimal Points. 25
3.3.3. On-column Analyte Mass 26
3.3.4. Mass Fractions and Concentrations 26
3.3.4.1. Dilution of a Solution Containing Multiple Analytes 26
3.3.4.2. Solution Created from Addition of Solutions 27
3.3.4.3. Conversion of Concentrations to Mass Fractions 28
3.4. Determination of Concentrations using Ion Chromatography 29

3.5. Determination of Mass Fractions using Combustion Ion Chromatography 30
3.6. Determination of Recoveries 31
3.7. Determination of Mass Fraction Ratios 31
3.8. Summary of Uncertainties Considered 32
4. Results 33
4.1. Instrument Response and Characterization of Partial Loop Injection System 33
4.2. Creation of Organofluorine and Organochlorine Calibration Curves 35
4.3. Fluoride Recovery of PFAS and Other Organofluorines 40
4.4. Effects of Cations on Fluorine Measurements 44
4.5. Concurrent Sulfur Determinations 45
5. Discussion 46
5.1. Recommended Best Practices 47
6. References 48
Appendix A. Reference Data 53
A.1. Values of Select NIST RM/SRMs 53
A.1.1. NIST SRM 1635a 53
A.1.2. NIST SRM 1646a 56
Appendix B. Equations 57
B.1. Definition of Variables 57
B.2. Linear Fit Uncertainty 57
B.3. 2nd Order Polynomial Fit Uncertainty 58
Appendix C. Analysis Code 59
C.1. Calibration Curve Creation and Uncertainty Calculations 59
C.2. Organofluorine and Organochlorine Calibration Curve 64
Appendix D. Additional Data and Figures 69
D.1. Sensitivity Figures 69
D.2. Output from Calibration Curve Fits 73
D.3. Example Chromatograph of NIST SRM Anions 76
D.4. Example Chromatograph of 3rd Party ISO-Certified and NIST-Traceable Anion Solution (ERA Custom Mix 3) 77
Appendix E. Effects of Glassware on Fluoride Measurements 78
Appendix F. List of Symbols, Abbreviations, and Acronyms 79

List of Tables

Table 1. Certified values of ERA Custom Anions Mix 3 standard solution. 8
Table 2. Certified values of NIST SRM anion standard solutions. 8
Table 3. Prepared solution containing approximately 100 mg/kg of each anion. 9
Table 4. Certified values of NIST SRM cation standard solutions. 9
Table 5. Certified mass fractions of 3rd-party standalone PFAS analytical standards. 10
Table 6. Non-certified mass fractions of each compound in NIST RM 8446. Note that NIST RM 8446 comes in two parts; part A contains only PFCAs, and part B contains PFCAs and PFOSA. 10
Table 7. Molecular formula, weight, and fluorine mass percentage of each 3rd party PFAS analytical standards. 11
Table 8. Molecular formula, weight, and fluorine mass percentage of each compound in NIST RM 8446. 11
Table 9. Certified elemental mass fractions of NIST SRM 2143 and 2144. 11
Table 10. Molecular formula, weight, and halogen mass percentage of NIST SRM 2143 and 2144. 11
Table 11. Certified mass fraction values (dry-mass basis) for SRM 1635a. 12
Table 12. Mass fraction value of interest (dry-mass basis) for SRM 1635a. 12
Table 13. SRM 1635a CANSPEX interlaboratory study results 12
Table 14. Certified values for NIST SRM 1646a 12
Table 15. IC injection volumes for each calibration level. 13
Table 16. Example analytical run table. 14
Table 17. Mass fractions of compounds and total fluorine mass fraction in solutions containing RM 8446 Part A 19
Table 18. Mass fractions of compounds and total fluorine mass fraction in solutions containing RM 8446 Part B. 19
Table 19. Mass fractions of certified elements in solutions containing SRM 2143 and SRM 2144. 20
Table 20. Mass fractions of lithium cation and fluoride anions in each solution (k=2). 21
Table 21. Mass fractions of calcium cation and fluoride anions in each solution (k=2). 21
Table 22. Maximum permissible errors allowed for nominal volumes between 1 mL to 2 mL. 23
Table 23. Maximum permissible errors allowed for nominal volumes between 2 mL to 5 mL. 23
Table 24. Maximum permissible errors allowed for nominal volumes between 5 mL to 25 mL. 23
Table 25. Technical specifications of the conductivity meter. 24
Table 26. Conductivity meter calibration parameters. 24
Table 27. 5-decimal analytical scale uncertainty values provided by manufacturer. 25
Table 28. Uncertainty components of masses weighed to 2 decimal points. 25
Table 29. Example dilution of a solution containing $\boldsymbol{n}$ analytes. 26
Table 30. Table containing five hypothetical solutions and their associated experimental parameters. 27

Table 31. Densities of solvents used in this report. 28
Table 32. Uncertainty budget for the determination of mass fraction ratios according to this report. 32
Table 33. IC injection volume and associated uncertainties estimated using fluoride calibration data (quadratic fit). 34
Table 34. CIC parameters for RM 8446 Part A. 35
Table 35. CIC parameters for RM 8446 Part B. 35
Table 36. CIC parameters for solutions containing both SRM 2143, 2144. 35
Table 37. CIC parameters for solution containing SRM 3182, 3183, 3184. 36
Table 38. Additional CIC parameters for solution containing SRM 3182, 3183, 3184. 36
Table 39. IC parameters for ERA Custom Mix 3. 36
Table 40. RM 8446 Part A fluoride mass fraction results (no blank correction). 40
Table 41. RM 8446 Part B fluoride mass fraction results (no blank correction). 40
Table 42. Averaged apparent fluoride concentration of adsorption solution of methanol blanks (N=4). 40
Table 43. RM 8446 Part A fluoride mass fraction results (with blank correction). 40
Table 44. RM 8446 Part B fluoride mass fraction results (with blank correction). 41
Table 45. Fluoride mass fractions and recovery percentages of 3rd-party PFAS standards (no blank correction). 41
Table 46. Fluoride mass fraction in solutions containing SRM 2143 and SRM 2144 (no blank correction). 42
Table 47. Chloride mass fraction in solutions containing SRM 2143 and SRM 2144 (no blank correction). 42
Table 48. Averaged apparent fluoride and chloride concentration of adsorption solution of water blanks (N=3). 42
Table 49. Fluoride mass fraction in solutions containing SRM 2143 and SRM 2144 (with blank correction). 43
Table 50. Chloride mass fraction in solutions containing SRM 2143 and SRM 2144 (with blank correction). 43
Table 51. Expected and measured mass fractions of lithium cation and fluoride anions (k=2). 44
Table 52. Expected and measured mass fractions of calcium cation and fluoride anions in each solution (k=2). 44
Table 53. Mass fractions of solid NIST SRMs using 100 mg/kg hydrogen peroxide in water as the absorber solution. 45
Table 54. Certified Mass Fraction Values (Dry-Mass Basis) for SRM 1635a. 53
Table 55. Non-Certified Mass Fraction Values (Dry-Mass Basis) for SRM 1635a. 54
Table 56. Mass Fraction Value of Interest (Dry Mass Basis) for SRM 1635a. 54
Table 57. Select Values from SRM 1635a CANSPEX Interlaboratory Study Results. 55
Table 58. Certified Values for NIST SRM 1646a. 56

Table 59. Noncertified values for NIST SRM 1646a. 56
Table 60. Fitting results from RM 8446 Part A. 73
Table 61. Fitting results from RM 8446 Part B. 73
Table 62. Fluoride fitting results from SRM 2143/2144. 73
Table 63. Chloride fitting results from SRM 2143/2144. 73
Table 64. Fluoride fitting results from direct injections. 74
Table 65. Fluoride fitting results from SRM 3183. 74
Table 66. Chloride fitting results from direct injections. 74
Table 67. Chloride fitting results from SRM 3182. 74
Table 68. Bromide fitting results from direct injections. 74
Table 69. Bromide fitting results from SRM 3184. 75
Table 70. Methanol blank values. 78

List of Figures

Figure 1. Illustration of the combustion oven module coupled with the autosampler and auto boat driver. 5

Figure 2. Illustration of a solid sample in a quartz boat being pyrohydrolyzed within a combustion tube. 5

Figure 3. Illustration of the various solutions used in CIC. 6

Figure 4. Illustration of the absorber module, with the name of each part (left) and path of the various fluid flows (right). 6

Figure 5. Illustration of the ion chromatograph module, with the name of each part (left) and path of the various fluid flows (right). 7

Figure 6. Fluoride sensitivities at different IC injection volume set points. Circles represent outliers, orange lines represent the median, boxes represent the first to third quartile of the data, and whiskers represent the farthest data point lying within the 1.5x the inter-quartile range. Outliers are defined as any data points that fall outside of the 1.5x the inter-quartile range. 33

Figure 7. Estimated IC injection volumes using fluoride calibration data (quadratic fit). 34

Figure 8. Fluoride calibration curves created using various standards. Dotted lines represent data extrapolation to the highest injected fluoride mass. 37

Figure 9. Chloride calibration curves created using various standards. Dotted lines represent data extrapolation to the highest injected chloride mass. 38

Figure 10. Bromide calibration curves created using various standards. Dotted lines represent data extrapolation to the highest injected bromide mass. 39

Figure 11. Fluoride recovery rates of RM 8446 with and without blank correction. 41

Figure 12. Fluoride recovery of 3rd-party PFAS standards (no blank correction). 42

Figure 13. Anion recovery rates of SRM 2143/2144 solutions. 43

Figure 14. Fluoride recoveries of lithium/calcium spiked samples (k=2, no blank correction). 44

Figure 15. Sensitivity of chloride and corresponding linear instrument response fit. 69

Figure 16. Sensitivity of bromide and corresponding linear instrument response fit. 70

Figure 17. Sensitivity of sulfate and corresponding linear instrument response fit. 71

Figure 18. Sensitivity of phosphate and corresponding linear instrument response fit. 72

Figure 19. Example chromatograph of a solution containing 1 mg/kg each of NIST SRM 3183 (Fluoride), 3182 (Chloride), 3184 (Bromide), 3186 (Phosphate), and 3181 (Sulfate). Retention times are listed in minutes. 76

Figure 20. Example chromatograph of anion solution (ERA Custom Mix 3) containing fluoride, chloride, nitrite, bromide, nitrate, phosphate, and sulfate. 77

Acknowledgments

We would like to thank the NIST Material Measurement Laboratory's Chemical Sciences Division and Office of Reference Materials for providing NIST Standard Reference Materials and Reference Materials used in this work.

Author Contributions

Halen D. Solomon: Conceptualization, Methodology, Investigation, Data curation, Writing-Original draft preparation, Visualization. **Andrew C. Maizel**: Conceptualization, Methodology, Investigation, Data curation. Writing-Reviewing and Editing. **Audrey F. Tombaugh**: Writing-Reviewing and Editing. **Brittany L. Stinger**: Writing-Reviewing and Editing. **Andre L. Thompson**: Writing- Reviewing and Editing, Supervision. **Rick D. Davis**: Funding Acquisition, Project Administration, Resources, Writing- Reviewing and Editing, Supervision.

1. Introduction

First responders are routinely exposed to halogenated and anthropogenic compounds like per- and polyfluoroalkyl substances (PFAS), polychlorinated biphenyls (PCBs), and polybrominated diphenyl ethers (PBDE) [1–4]. This is particularly true for those responding to fire scenes, where they may be exposed to these compounds from various sources, such as applied coatings on turnout gear [5–9], volatilized compounds in combustion fumes [10], and dissolved halogenated compounds in fire suppression foams [11]. Many of these halogenated compounds have suspected health concerns, such as immunosuppression, genotoxicity, and neurotoxicity [12–18].

Halogenated compounds are most often identified and measured using mass spectrometry coupled with chromatography. Targeted analysis provides the most accurate characterization of specifics PFAS compounds because it relies on a defined list of analytes and calibration with appropriate PFAS standards [19–21]. When a commercial PFAS calibration standard isn't available, a chemically similar standard may be used, but that adds an additional uncertainty to the measured value. While highly accurate, the targeted approach is expensive due to the high cost of the calibration standards and limits the PFAS to those with commercially available calibration standards. Non-targeted analysis can help identify a broader range of species because it does not require compound-specific standards, but it is not typically quantitative and depends heavily on the data-processing algorithms and the quality of the spectral database. Both targeted and non-targeted approaches commonly use liquid chromatography coupled with mass spectrometry [6, 22, 23] and often require significant sample preparation to remove matrix interferences and extract or concentrate the analytes of interest [24–27].

Combustion ion chromatography (CIC) is an alternative method for elemental analysis of solid, liquid, and some gaseous samples [28–30]. In CIC, samples are digested by pyrohydrolysis, and the resulting volatile elements and compounds are collected and measured by ion chromatography. For halogenated materials, this provides total halogen mass fractions rather than compound-specific information. Although the identities of individual compounds are lost during combustion, CIC can be a useful screening tool for identifying samples with elevated halogen content. This is especially useful for PFAS-related measurements because CIC does not depend on compound-specific analytical standards or prior knowledge of newly emerging or unknown PFAS species.

Understanding the strengths and limitations of CIC for fluorine and halogen measurements is important across several applications. In semiconductor manufacturing and photolithographic applications, for example, both organic and inorganic forms of fluorine may contribute to total fluorine measurements, which complicates interpretation [31–35]. In other scenarios, such as fire-scene investigations involving lithium-ion battery systems, elevated cation concentrations may also need to be considered [36]. These issues have been noted in the literature but have not been thoroughly investigated [37, 38].

This publication describes and characterizes a CIC method for determining fluorine, chlorine, bromine, and sulfur through measurement of pyrohydrolysis products: F^-, Cl^-, Br^-, and SO_4^{2-}. We examine blank corrections and the use of non-linear calibration curves to reduce measurement uncertainty. The method is then applied to selected NIST Standard Reference Materials (SRM)

and Reference Materials (RM), with measured elemental mass fractions compared against reported or certified values. We also evaluate the potential effects of lithium and calcium cations on fluoride measurements. Finally, we report overall halogen recovery values for PFAS and non-PFAS compounds, including p-fluorobenzoic acid and m-chlorobenzoic acid.

2. Materials and Methods

2.1. Consumables Preparation and Instrument Setup

High-performance liquid chromatography (HPLC) vials (2 mL capacity, amber vials), glass inserts (250 µL), and 2 mL vial caps with polytetrafluoroethylene (PTFE)/silicone septa were obtained from Agilent Technologies (Santa Clara, CA).[1] HPLC-grade methanol was obtained from Fisher Scientific (Hampton, NH). Ultra-high-purity (UHP) argon and UHP oxygen (both 99.999 % purity) were obtained from Roberts Oxygen (Rockville, MD). Combustion boats, quartz tubes, and columns were obtained from Metrohm AG (Herisau, Switzerland).

To reduce fluoride background levels, all glassware including glass inserts were rinsed with HPLC-grade methanol, then triple-rinsed with ultra-pure water (UPW, water with 18.2 MΩ or higher resistance). The rinsed glassware was dried under a flow of UHP nitrogen then either used immediately or placed into a desiccator until used to avoid the absorption of fluorinated compounds from ambient air.

Samples were placed inside of combustion boats. Combustion boats of size 40 mm x 9 mm made of either quartz or ceramic were used in this study. For solid samples, 6 mm x 18 mm quartz tubes and quartz wool were used to fix small samples in place within the combustion boat if needed. All combustion boats, quartz tubes, quartz wool, and quartz filters were soaked in HPLC-grade methanol for a minimum of one hour prior to baking out. All materials were baked out at 1050 °C for 5 min prior to use in sample combustion. Samples of masses between 0.1 mg and 110 mg were then loaded onto the combustion boat for analysis.

For liquid samples, approximately 100 µL of liquid samples were dispensed into glass inserts of 250 µL volume, which were then placed into a HPLC vial of 2 mL volume. HPLC vials were then capped with resealable HPLC caps. In addition, quartz filters of 47 mm diameter and 432 µm thickness (PALL Life Sciences, Port Washington, NY) were cut to approximately 18 mm by 9 mm rectangles. Cut filters were fitted inside combustion boats and baked out at 1050 °C for 5 min.

Pyrohydrolysis was performed in a quartz combustion tube, with a flow of 300 mL/min of UHP O_2 and 100 mL/min of UHP Ar. For solid samples, the autosampler was equipped with a boat gripper to place combustion boats containing pre-weighed samples into the combustion tube by placing the boat onto an automatic boat driver (ABD) equipped with a quartz hook. For liquid samples, an automatic sampler was equipped with a metering syringe of either 100 µL or 50 µL capacity. The automatic sampler injected a preset volume of sample through a silicone septum onto a combustion boat fitted with a quartz filter, which rested on the ABD quartz hook. The metering syringes used were rinsed with HPLC-grade methanol three times before and after each sample injection.

The eluent used for the ion chromatography system consisted of 3.2 mM Na_2CO_3 and 1 mM $NaHCO_3$ dissolved in UPW and was obtained as a 20X concentrate from Metrohm AG

[1] Certain equipment, instruments, software, or materials, commercial or non-commercial, are identified in this paper in order to specify the experimental procedure adequately. Such identification does not imply recommendation or endorsement of any product or service by NIST, nor does it imply that the materials or equipment identified are necessarily the best available for the purpose.

(Herisau, Switzerland). Eluent flow rate was set to 0.7 mL/min ± 0.0001 mL/min.[2] Absorber solution consisting of 0.5 mg of H_2O_2 per kg of UPW was used to collect the combustion gases from the combustion module. UPW was used to rinse out the sample loop, as well as to aid in oxidization within the combustion tube by humidifying the gas flow. Water inlet rate was set to 0.1 mL/min for the entire combustion duration. The total volume of water dispensed into the combustion tube was recorded by the motorized burette. The feed rate and combustion duration were dynamically determined by a light-intensity sensor connected to the combustion tube, ensuring complete combustion while minimizing experimental delays.

Trap columns (Metrohm Metrosep A Trap 1 – 100/4.0 and Metrohm Metrosep I Trap 1 – 100/4.0) were used to retain ions from the absorber solution and UPW, respectively. A preset volume ranging from 4 µL to 200 µL of the absorption solution (solution containing the dissolved ions) was injected from the absorber module into the ion chromatograph (IC). A preconcentrator column (Metrohm Metrosep A PCC 2 HC/4.0) was used to concentrate anions of interest and to reduce matrix effects, including peroxide-related effects. A guard column (Metrohm Metrosep A Supp 5 Guard/4.0) protected the analytical (separation) column (Metrohm Metrosep A Supp 5 - 150/4.0). The analytical column was kept at 30 °C ± 0.2 °C during the entirety of analysis.[2] The outlet of the analytical column was connected to a chemical suppression module that captured cations and replaced them with protons to reduce the background conductivity. The chemical suppression module was regenerated with 1.2 mL of 0.5 M H_2SO_4 solution dispensed by a motorized burette between every injection. The chemical suppression modules were connected to a CO_2 suppression module that removes carbonic acid to further reduce the background conductivity.

Analytes were detected with a conductivity detector (Metrohm IC Conductivity Sensor 2.850.9010). Peaks were identified and integrated using the vendor's peak-picking algorithm with a peak area threshold of 0.01 µS*min/cm. Peak retention times were verified using NIST SRMs.

[2] Uncertainty values were obtained from the instrument manufacturer.

2.1.1. Illustrative Guide

This section is an illustrative guide of the instrumental method.

Figure 1 is an illustration of the general workflow of the combustion oven module. The only difference between liquids and solids is loading the test sample. For solids, the sample is placed in a quartz boat, the boat is loaded into the combustion tube using autosampler and auto boat driver. For liquids, liquid test sample is loaded into a HPLC vial, which dispenses the liquid into the quartz boat before it is loaded into the combustion tube.

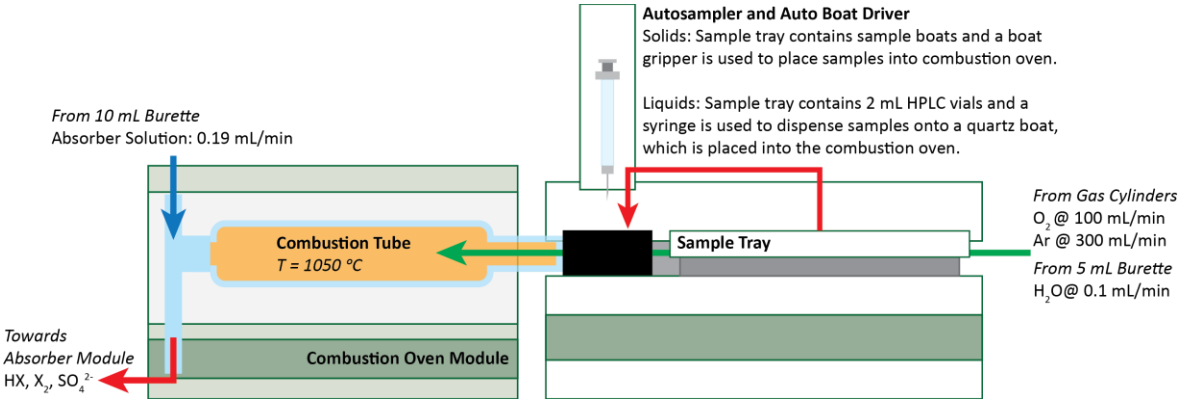

Figure 1. Illustration of the combustion oven module coupled with the autosampler and auto boat driver.

Figure 2 shows a solid sample placed in a quartz boat, which is attached to a quartz hook. The combustion tube is kept at 1050 °C, with oxygen, argon, and water vapor continuously flowing into the tube. In this environment, the sample is pyrohydrolyzed (heated in the presence of steam), and the combustion vapor is collected through dissolution into the absorber solution.

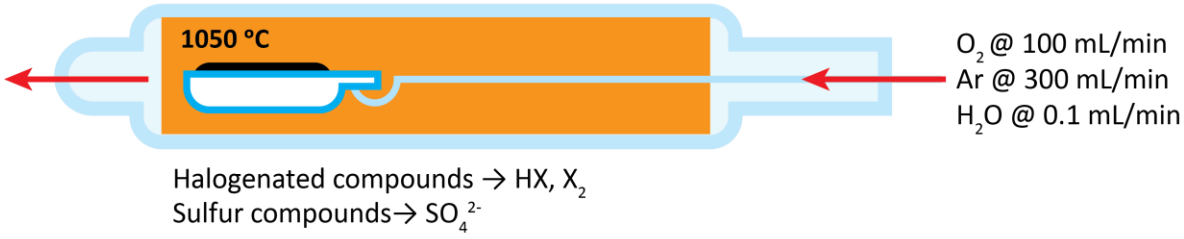

Figure 2. Illustration of a solid sample in a quartz boat being pyrohydrolyzed within a combustion tube.

Figures 3 and 4 are the four solutions used in the operation of the instrument and an illustration of them in the general workflow of the absorber module. The left side **Figure 4** displays the key components, including the 6-port and 10-part valves, which direct the flow of solutions throughout the module, the trap columns that retain ions from prepared solutions, and the solution-dispensing burettes. The right side shows the connections between components and valves.

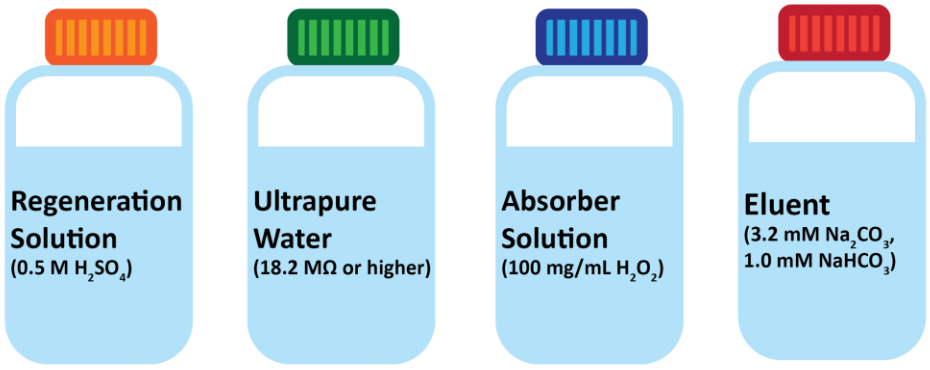

Figure 3. Illustration of the various solutions used in CIC.

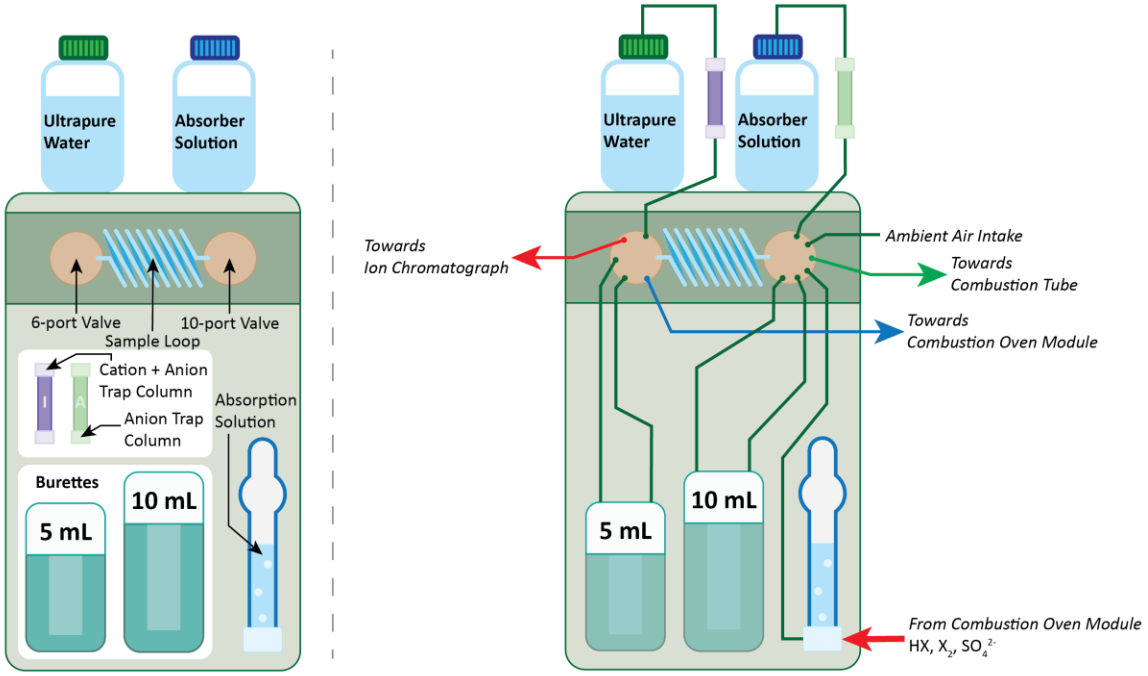

Figure 4. Illustration of the absorber module, with the name of each part (left) and path of the various fluid flows (right).

Figure 5 is an illustration of the general workflow of the solutions in **Figure 3** in the ion chromatograph module. The left side of the figure displays the key components, including the 6-port valve, which direct the flow of various solutions throughout the module, the preconcentration column, the analytical and guard columns (displayed as one unit), and the 2 mL burette that dispenses the regeneration solution. The cation exchanger shown in the figure is chemical suppression module mentioned in the previous section. The right side of **Figure 5** shows the connections between the various components and the valve, and the connection between the ion chromatograph module and the absorber module.

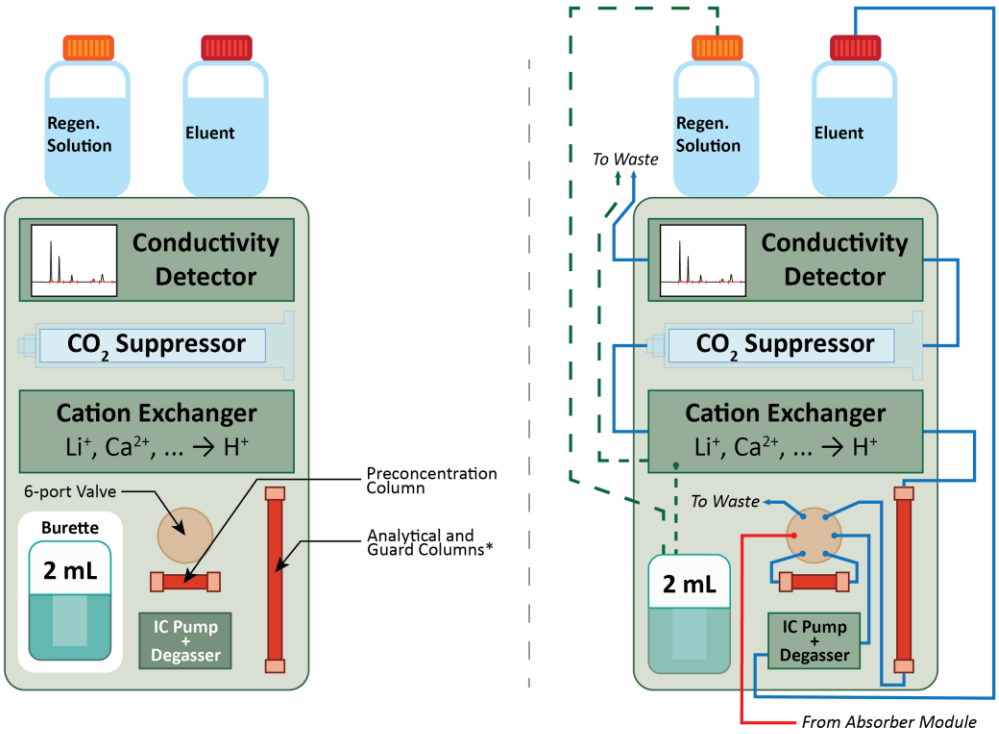

Figure 5. Illustration of the ion chromatograph module, with the name of each part (left) and path of the various fluid flows (right).

2.2. Reference Materials and Analytical Standards

External calibration curves were created using an ISO-certified and NIST-traceable anion solution (ERA Custom Mix 3 – REAIC1035, Waters ERA, Golden, CO) containing 100 mg/kg each of F^-, Cl^-, NO_2^-, NO_3^-, Br^-, PO_4^-, and SO_4^-, which was diluted to approximately 2 mg/kg using UPW. The certified values and the corresponding expanded uncertainty values reported by the manufacturer for the initial anion solution are in **Table 1**. An example chromatograph is provided in **Appendix D.4**.

Table 1. Certified values of ERA Custom Anions Mix 3 standard solution.

ERA Custom Anions Mix 3 (Lot # 631022m, Expiration Date: Oct. 18th, 2025[3])		
Anion	**Certified Value (mg/L)**	**Expanded Uncertainty (k=2, mg/L)**
F^-	100	1.09
Cl^-	100	0.960
NO_2^-	100	0.750
NO_3^-	100	3.33
Br^-	100	2.94
PO_4^{3-}	100	0.546
SO_4^{2-}	100	1.18

A solution containing approximately 1 mg/kg each of SO_4^-, Cl^-, F^-, Br^-, and PO_4^- was created by combining NIST SRM 3181, 3182, 3183, 3184, and 3186. The resulting solution was injected into the IC to confirm the retention times of each analyte and to verify the validity of the calibration curves during analytical runs. The same solution was also used to study the combustion efficiencies of anions. The certified anion mass fraction values and the reported expanded uncertainties for each NIST SRM are listed in **Table 2** and in the referenced documents [39–43]. A chromatograph of a solution containing approximately 1 mg/kg of each NIST SRM anion can be found in **Appendix D.3**.

Table 2. Certified values of NIST SRM anion standard solutions.

NIST SRM Anion Standard Solutions				
SRM Number	**SRM Information**Error! Bookmark not defined.	**Anion**	**Certified Value (mg/g)**	**Expanded Uncertainty (k=2, mg/g)**
3183	Lot # 140203 Exp. Dec. 31st, 2027	F^-	0.9968	3.1×10^{-3}
3182	Lot # 190830 Exp. Mar. 31st, 2032	Cl^-	1.0040	1.9×10^{-3}
3184	Lot # 151130 Exp. Apr. 30th, 2028	Br^-	0.9993	2.3×10^{-3}
3186	Lot # 170606, Exp. Jun. 30th, 2025	PO_4^{3-}	1.0005	4.1×10^{-3}
3181	Lot # 080603 Exp. Dec. 31st, 2025	SO_4	1.0000	1.6×10^{-3}

[3] Solutions were used prior to their expiration dates.

NIST SRMs were combined into one solution using UPW to create a master stock solution containing approximately 100 mg/kg of each anion standard. The final anion mass fraction values are provided in **Table 3**. Uncertainties were calculated by following the procedure described in **Section 3.3.4.2**.

Table 3. Prepared solution containing approximately 100 mg/kg of each anion.

Master Stock Solution Containing NIST SRM Anion Standards			
SRM Number	**Anion**	**Calculated Value (mg/kg)**	**Expanded Uncertainty (k=2, mg/kg)**
3183	F^-	99.20	0.05
3182	Cl^-	99.66	0.05
3184	Br^-	99.60	0.05
3186	PO_4^{3-}	100.8	0.05
3181	SO_4	99.58	0.05

NIST SRM 3129a (lithium standard solution) and 3109a (calcium standard solution) were used to characterize the effect cations may have on fluoride mass fraction measurements. The certified elemental mass fraction for each NIST SRM are provided in **Table 4** and referenced in documents [44, 45].

Table 4. Certified values of NIST SRM cation standard solutions.

NIST SRM Cation Standard Solutions				
SRM Number	**SRM Information**Error! Bookmark not defined.	**Cation**	**Certified Value (mg/g)**	**Expanded Uncertainty (k=2, mg/g)**
3129a	Lot # 100714 Exp. Mar. 31st, 2029	Li^+	9.969	0.030
3109a	Lot # 130213 Exp. Nov. 1st, 2025	Ca^{2+}	9.819	0.019

Third-party PFAS standards 2-perfluorobutyl ethanol (4:2 FTOH), 1-perfluoropentyl ethanol (5:2 sFTOH), 2-perfluorooctyl ethanol (8:2 FTOH), 2-perfluorooctyl ethanol (10:2 FTOH), and 1H, 1H, 2H, 2H-perfluorodecyl acrylate (8:2 FTAcr), and NIST RM 8446 (Perfluorinated carboxylic acids and perfluorooctane sulfonamide in methanol) were used to characterize organofluorine combustion efficiencies. Each standard was certified for the compound mass fraction. Detailed information regarding the concentration and purity for 3rd-party standalone PFAS standards are provided in **Table 5**. Chemical Abstracts Service (CAS) Registry Numbers are provided in **Appendix F**.

Table 5. Certified mass fractions of 3rd-party standalone PFAS analytical standards.

3rd-party PFAS Analytical Standards					
Compound Abbr.	**Compound**	**Vendor / Lot #**	**Certified Value (mg/L)**	**Expanded Uncertainty (k=2, mg/L)**	**Solvent**
4:2 FTOH	2-Perfluorobutyl ethanol	Wellington Laboratories FBET0419	50.0	2.5	Methanol
5:2 sFTOH	1-Perfluoropentyl ethanol	Wellington Laboratories 52sFTOH0115	50.0	2.5	Methanol
8:2 FTOH	2-Perfluorooctyl ethanol	Wellington Laboratories FOET 0221	50.0	2.5	Methanol
10:2 FTOH	2-Perfluorodecyl ethanol	Wellington Laboratories FDET0920	50.0	2.5	Methanol
8:2 FTAcr	1H, 1H, 2H, 2H-Perfluorodecyl acrylate	Wellington Laboratories 82FTAcr1020	50.0	2.5	Isooctane

NIST RM 8446 Part A and Part B were separately used to create PFAS-based calibration standards. More information regarding the preparation and characterization methods are presented in the referenced document [46] and in **Tables 6-8**. **Equation 1** was used to calculate the mass percentage of fluorine of each compound in **Tables 7 and 8**.

Table 6. Non-certified mass fractions of each compound in NIST RM 8446. Note that NIST RM 8446 comes in two parts; part A contains only PFCAs, and part B contains PFCAs and PFOSA.

NIST RM 8446 – Perfluorinated Carboxylic Acids and Perfluorooctane Sulfonamide in Methanol			
Lot #: N/A, Expiration Date: Jan. 31st, 2034			
Compound Abbr.	**Compound**	**Value (mg/g)**	**Expanded Uncertainty (k=2, mg/g)**
PFCAs in Methanol Part A			
PFHxA	Perfluorohexanoic acid	59.1	1.4
PFHpA	Perfluoroheptanoic acid	76.0	7.2
PFOA	Perfluorooctanoic acid	54.8	2.2
PFNA	Perfluorononanoic acid	63.0	1.4
PFDA	Perfluorodecanoic acid	58.1	4.0
PFUnA	Perlfuoroundecanoic acid	62.8	6.5
PFDoA	Perfluorododecanoic acid	59.5	7.0
PFTriA	Perfluorotridecanoic acid	62.9	2.8
PFTA	Perfluorotetradecanoic acid	58.0	3.8
PFCAs and PFOSA in Methanol Part B			
PFBA	Perfluorobutanoic acid	43	11
PFPeA	Perfluoropentanoic acid	60.9	0.9
PFOSA	Perfluorooctane sulfonamide	66.9	1.7

In **Equation 1**, the molecular formula and the molecular weight (MW) were used to calculate the fluorine mass percent composition of each compound. n_F is the number of fluorine atoms in each compound while 18.998 is the atomic mass of fluorine.

$$\text{Mass \% of fluorine (\%)} = \frac{n_F \times 18.998}{\text{MW}} \times 100 \quad (1)$$

Table 7. Molecular formula, weight, and fluorine mass percentage of each 3rd party PFAS analytical standards.

3rd Party PFAS Analytical Standards			
Compound Abbr.	**Molecular Formula**	**Molecular Weight (g/mol)**	**Mass % of Fluorine**
4:2 FTOH	$C_6H_5F_9O$	264.09	64.75
5:2 sFTOH	$C_7H_5F_{11}O$	314.1	66.53
8:2 FTOH	$C_{10}H_5F_{17}O$	464.12	69.59
10:2 FTOH	$C_{12}H_5F_{21}O$	564.13	70.72
8:2 FTAcr	$C_{13}H_7F_{17}O_2$	518.169	62.33

Table 8. Molecular formula, weight, and fluorine mass percentage of each compound in NIST RM 8446.

NIST RM 8446 – Perfluorinated Carboxylic Acids and Perfluorooctane Sulfonamide in Methanol			
Analyte	**Molecular Formula**	**Molecular Weight (g/mol)**	**Mass % of Fluorine**
PFCAs in Methanol Part A			
PFHxA	$C_6HF_{11}O_2$	314.05	66.55
PFHpA	$C_7HF_{13}O_2$	364.06	67.84
PFOA	$C_8HF_{15}O_2$	414.07	68.82
PFNA	$C_9HF_{17}O_2$	464.08	69.60
PFDA	$C_{10}HF_{19}O_2$	514.08	70.22
PFUnA	$C_{11}HF_{21}O_2$	564.09	70.73
PFDoA	$C_{12}HF_{23}O_2$	614.10	71.76
PFTriA	$C_{13}HF_{25}O_2$	664.10	71.52
PFTA	$C_{14}HF_{27}O_2$	714.11	71.83
PFCAs and PFOSA in Methanol Part B			
PFBA	$C_4HF_7O_2$	214.04	62.13
PFPeA	$C_5HF_9O_2$	264.05	64.76
PFOSA	$C_8H_2F_{17}NO_2S$	499.15	64.71

NIST SRMs 2143 (p-fluorobenzoic acid) and 2144 (m-chlorobenzoic acid) were used to verify the accuracy of fluorine and chlorine mass fraction measurements. Each SRM was certified for their elemental mass fraction (i.e. fluorine for SRM 2143, chlorine for SRM 2144) [47, 48]. **Tables 9 and 10** contain their certified elemental mass fractions and associated chemical properties.

Table 9. Certified elemental mass fractions of NIST SRM 2143 and 2144.

High-purity NIST SRMs				
SRM Number	**SRM Information**	**Compound**	**Certified Value**	**Expanded Uncertainty (k=2)**
2143	Lot # N/A Exp. Mar. 31st, 2029	p-Fluorobenzoic acid	9.969 F mg/g	0.030 F mg/g
2144	Lot # N/A Exp. Nov. 1st, 2025[4]	m-Chlorobenzoic acid	9.819 Cl mg/g	0.019 Cl mg/g

Table 10. Molecular formula, weight, and halogen mass percentage of NIST SRM 2143 and 2144.

High-purity NIST SRMs				
SRM Number	**Compound**	**Molecular Formula**	**Molecular Weight (g/mol)**	**Mass % Element**
2143	p-Fluorobenzoic acid	$C_7H_5FO_2$	140.11	0.030 F mg/g
2144	m-Chlorobenzoic acid	$C_7H_5ClO_2$	156.56	0.019 Cl mg/g

[4] Solution was used prior to its expiration date.

NIST SRM 1635a and 1646a were used to for calibrating for measuring fluoride and sulfur mass fractions in solid matrices [49, 50]. **Tables 11-14** show values used in this report. More information regarding these SRMs is provided in **Appendix A**.

Table 11. Certified mass fraction values (dry-mass basis) for SRM 1635a.

Element	Constituent Type	Certified Value (mg/kg)	Expanded Uncertainty (k=2, mg/kg)
Sulfur (S)	Minor	2909	80

Table 12. Mass fraction value of interest (dry-mass basis) for SRM 1635a.

Element	Value (mg/kg)
Bromine (Br)	1

Table 13. SRM 1635a CANSPEX interlaboratory study results.

Parameter	Most Likely Value	95 % Coverage Interval of Mean Value	Pooled Within Lab Standard Deviation (s_w)	Pooled Between Lab Standard Deviation (s_B)	Total Number of Labs
Total Sulfur % dry basis	0.294	6×10^{-3}	8×10^{-3}	0.022	112
Chlorine µg/g dry basis	51	19	8	41	41
Fluorine µg/g dry basis	63	11	5	22	31

Table 14. Certified values for NIST SRM 1646a.

Element	Certified Value (mg/kg)	Expanded Uncertainty (k=2, mg/kg)
Phosphorus (P)	270	10
Sulfur (S)	3520	40

2.3. Analytical Run Setup

Analytical runs consisted of two calibration curves, IC injections of NIST SRMs, combustion of NIST SRMs, boat blanks/carryover checks, and mid-level calibration curve validity checks (CCV). Reported values are from a minimum of triplicate analytical runs.

Calibration curves were created by the direct IC injection of the 2 mg/kg solution containing F^-, Cl^-, NO_2^-, NO_3^-, Br^-, PO_4^-, and SO_4^-. Each level was created by the injection of various volumes of the solution. **Table 15** shows each level and the corresponding IC injection volume. Cal 4 was used solely as CCVs and was not considered when creating a calibration curve.

Table 15. IC injection volumes for each calibration level.

Calibration Level	IC injection volume (µL)
Cal 1	200
Cal 2	100
Cal 4	50
Cal 5	40
Cal 10	20
Cal 20	10
Cal 50	4

1. Calibration curve: Each run contained two sets of calibration curves, one at the start of the analytical run and one at the end of the analytical run. The two sets of calibration curves were considered simultaneously (i.e., two data points per calibration level) during the instrument response curve fitting.
2. Direct IC injection of NIST SRMs: A solution containing approximately 1 mg/kg of NIST SRM 3181, 3182, 3183, 3184, and 3186 is directly injected into the IC. All runs were performed in duplicate, and each run is valid only if the recoveries fall between 80 % to 120 % (same criterion as calibration curve validity checks). IC injection volume was set to 200 µL.
3. Combustion of NIST SRMs: For liquid sample analytical runs, 50 µL of a solution containing approximately 100 mg/kg of NIST SRM 3181, 3182, 3183, 3184, and 3186 was combusted. For solid sample analytical runs, NIST SRM 1635a and 1646a were used to confirm fluorine and sulfur determinations. IC injection volume was set to 200 µL.
4. Boat blank/carryover checks: Empty boats were combusted in triplicate or more to ensure minimal background contamination. Empty boats were combusted every 10 sample analyses to serve as a carryover check. IC injection volume was set to match the sample IC injection volumes. If more than one IC injection volume is present in a run, empty boats were combusted at each IC injection volume.
5. Matrix/method and solvent blanks: Matrix/method blanks refer to the combustion of materials intrinsically related to the preparation of the sample. For example, adsorbable organofluorine (AOF) determinations typically utilize activated carbon as the absorbent. The pristine activated carbon itself may contain background levels of halogens, and therefore such background levels must be removed from any AOF mass fractions. Another

example would be the dilution of PFAS solutions using solvents such as methanol and ethyl acetate. The solvents themselves may contain background levels of halogens, and such backgrounds should be removed during determination of PFAS mass fractions.

Depending on the sample preparation method, a matrix/method blank or solvent blank was prepared to perform blank corrections. Blanks were analyzed at least in triplicate and matched both the IC injection volumes and combustion masses of the samples. If multiple IC injection volumes and combustion masses were used, triplicates of blanks were prepared for each IC injection volume/combustion mass combination.

For liquids, the solvents used to dilute samples were used as blanks (for example, methanol for PFAS compounds). For solids such as NIST SRM 1635a and 1646a, matrix blanks were not considered, as it is difficult to define the appropriate blank material.

6. Samples: Samples were analyzed in at least triplicate. The IC injection volume was kept constant for all replicates. Replicate combustion masses had a relative standard deviation (RSD) of less than 20 %.
7. Calibration curve validity (CCV) checks: A mid-level calibration standard was analyzed every 10 samples. The analytical run was considered valid only when all measured mid-level calibration standard recoveries were within 80 % to 120 %.

An example analytical run table with 30 samples of one matrix type is in **Table 16**.

Table 16. Example analytical run table.

1st Calibration Curve
NIST SRM Direct IC Injection
NIST SRM Combustion Check
Boat Blank 1
Matrix Blank 1
Samples 1-10
Boat Blank 2
CCV 1
Matrix Blank 2
Samples 11-20
Boat Blank 3
CCV 2
Matrix Blank 3
Samples 21-30
NIST SRM Direct IC Injection
2nd Calibration Curve

2.4. Instrument Response and the Characterization of Partial Loop Injection System

To create calibration curves, the instrument response for each analyte must be known. Instrument response was explored by defining a sensitivity parameter, S. It was defined as the peak area (A) divided by the mass of the analyte (m) injected into the column (**Equation 2**).

$$S = \frac{A}{m} \tag{2}$$

A linear and quadratic instrument response were considered, where a_2, a_1, and a_0 are fitting constants (**Equations 3 and 4**).

$$A = a_2 m^2 + a_1 m + a_0 \tag{3}$$

$$A = a_1 m + a_0 \tag{4}$$

Sensitivities for each instrument response model were calculated. **Equation 5** shows the sensitivity of an instrument that shows a perfect linear response.

$$S = \frac{A}{m} = \frac{a_1 m + a_0}{m} = a_1 + \frac{a_0}{m} \tag{5}$$

Similarly, the sensitivity can be expressed as seen in **Equation 6** for a perfect quadratic instrument response.

$$S = \frac{A}{m} = \frac{a_2 m^2 + a_1 m + a_0}{m} = a_2 m + a_1 + \frac{a_0}{m} \tag{6}$$

Valid calibration data over 5 months (N = 34) were collected and fitted to **Equations 5 and 6** for each analyte.

There are two injection systems: full-loop and partial-loop. Full-loop injection systems maximize volume reproducibility by completely filling the loop but require physical loop replacement to alter injection volumes. In contrast, partial-loop injection systems utilize an external metering device to aspirate samples into only a portion of the loop. This allows for a wider quantifiable mass fraction range than the full-loop injection system as the injection volume can be adjusted. The ability to adjust the volume can then be used to ensure the loaded mass of analyte remains within the method quantification range. However, this approach introduces new sources of uncertainty in the final quantification.

Here, a partial-loop injection system was used to inject the absorption solution (solution that contains analytes of interest originating from the pyrohydrolysis process) into the ion chromatograph. To characterize the variability of the partial loop injection system, valid calibration data over 5 months were collected and fitted to a calibration model (**Equations 7 and 8**), where c is the concentration of the solution being injected into the IC, V is the volume of the solution being injected into the IC (referred henceforth as the IC injection volume), and a_2, a_1, a_0 are fitting parameters. The fitting parameters were calculated using a Python-based curve fitting package (LMFIT) [51].

$$A = a_2 (cV)^2 + a_1 (cV) + a_0 \tag{7}$$

$$A = a_1 (cV) + a_0 \tag{8}$$

The IC injection volume uncertainty U_V was estimated by first using **Equations 7 and 8** to calculate the estimated IC injection volume and using the standard deviation of the estimated volumes as the uncertainty (**Equations 9 and 10**).

It is worth noting that the peak area uncertainties can be affected by various outside factors, such as temperature variations of the column, variations in the strength of the eluent, pressure variations in the eluent pump, and cell temperature of the conductivity sensor. Some of these external factors have been examined in literature for other chromatography-based measurements [52–55]. The response was modeled using either a linear or quadratic fit. As such, the uncertainty derived from this section is only an approximation and could be examined further with other methods. In this manuscript, we utilized this simpler method as dedicated experimental design of each external factor would have required both a significant modification of the existing hardware and additional, dedicated methods for measuring each factor.

$$V = \frac{-a_1 c \pm \sqrt{(a_1 c)^2 - 4(a_0 - A)a_2 c^2}}{2a_2 c^2} \tag{9}$$

$$V = \frac{A - a_0}{a_1 c} \tag{10}$$

2.5. Blank Subtraction and Determination of Halogen Mass Fractions

2.5.1. Determination of Halogen Mass Fractions

Determination of halogen mass fractions was performed using two related but separate methods: IC injection of liquids as-is into the ion chromatograph (direct injection) and IC injection of pyrohydrolyzed samples (combustion ion chromatography).

2.5.1.1. Concentration and Mass Fraction Using Direct Injection

The concentration (and by extension, its mass fraction) of halides in liquid samples (γ_{sample}) is determined by directly injecting a portion of the solution into the IC (**Equation 11**). Determination of halogen concentrations requires the knowledge of both the on-column analyte mass (m_{column}) and IC injection volume (V_{IC}).

$$\gamma_{sample} = \frac{m_{column}}{V_{IC}} \tag{11}$$

With the solvent density ($\rho_{solvent}$), the mass fraction is calculated using **Equation 12**.

$$w_{sample} = \frac{\gamma_{sample}}{\rho_{solvent}} \tag{12}$$

2.5.1.2. Mass Fraction Using Combustion Ion Chromatography

The determination of mass fraction (w_{sample}) requires two additional variables as seen in **Equation 13**: the total volume of the absorption solution ($V_{absorption}$) and the mass of the combusted ($m_{combustion}$).

$$w_{sample} = \frac{m_{column}}{V_{IC}} \times \frac{V_{absorption}}{m_{combustion}} \tag{13}$$

When the sample is analyzed more than once, the arithmetic average mass fraction ($\overline{w}_{sample}$) was calculated using **Equation 14**.

$$\overline{w}_{sample} = \frac{\sum w_{replicate}}{n} \tag{14}$$

2.5.1.3. Blank Subtraction

Blank subtraction eliminates background signals, instrument noise, and baseline drift, ensuring accurate peak identification and improved accuracy and reproducibility in halogens and sulfur measurements. Blank subtraction was performed based on the availability of matrix/methods blanks or solvent blanks. For solids and liquids without appropriate matrix blanks, boat blank subtractions were performed. This was done by combusting empty boats in triplicates or more with the same IC injection volumes as the samples, then subtracting the blank boat absorption solution halogen concentration from the sample absorption solution halogen concentration

(**Equation 15**). $w_{sample_{bc}}$ denotes blank-subtracted sample mass fractions and $w_{sample_{nc}}$ denotes non-corrected sample mass fractions.

$$w_{sample_{bc}} = \frac{\left(m_{column} \times V_{absorption}\right)_{sample} - \left(m_{column} \times V_{absorption}\right)_{blank}}{V_{IC} \times m_{combustion}} \quad (15)$$

If matrix blanks were available (for example, pristine activated carbon for adsorbable organofluorine determinations), the mass fraction values of the matrix w_{matrix} were subtracted from the measured non-corrected sample mass fraction values $w_{sample_{nc}}$. If dilutions were performed, it was assumed that the solvent(s) used were an appropriate matrix blank (**Equation 16**).

$$w_{sample_{bc}} = w_{sample_{nc}} - w_{matrix} \quad (16)$$

Both non-blank corrected and blank corrected values were reported throughout this report and are clearly noted as such.

2.5.1.4. Limit of Determination and Limit of Quantitation

Limit of determination (LOD) and Limit of quantitation (LOQ) are foundational benchmarks in analytical chemistry. They define the lowest concentration of a substance that an analytical procedure can reliably distinguish from zero (LOD) and measure with acceptable accuracy and precision (LOQ).

LOD is per IC injection volume (V_{IC}). For each V_{IC} present within the analytical run, a minimum of three replicates of blank boats with the same V_{IC} was combusted. Since the calibration curve was created using direct IC injections while blanks were determined based on combustion IC, the on-column analyte mass was used to determine the LOD per analytical run. Averages of sample on-column analyte mass $\bar{m}_{sample}$ must be higher than three times the maximum value between the average of the blank boat on-column analyte mass $\bar{m}_{blank}$ or the standard deviation of the blank boat on-column analyte mass σ_{blank}in order to be reportable (**Equation 17**).

$$\bar{m}_{sample} > \max(3\bar{m}_{blank}, 3\sigma_{blank}) \quad (17)$$

LOQ is also per V_{IC} value. For each V_{IC} present within the analytical run, a minimum of three replicates of blank boats with the same V_{IC} were combusted. Since the calibration curve was created using direct IC injections while blanks were determined based on combustion IC, the on-column analyte mass was used to determine the LOQ per analytical run. Averages of sample on-column analyte mass $\bar{m}_{sample}$ must be higher than three times the maximum value between the average of the blank boat on-column analyte mass $\bar{m}_{blank}$ or the standard deviation of the blank boat on-column analyte mass σ_{blank} plus the average on-column analyte mass of the lowest calibration level $\bar{m}_{lc}$ (**Equation 18**).

$$\bar{m}_{sample} > \bar{m}_{lc} + \max(3\bar{m}_{blank}, 3\sigma_{blank}) \quad (18)$$

2.6. Organofluorine and Organochlorine Calibration Curve Creation using NIST RM 8446, NIST SRM 2143 and 2144

Organofluorine and organochlorine calibration curves were created by combusting a series of solutions containing NIST SRM 2143 and 2144. Additional organofluorine calibration curves were also created using the NIST RM 8446 Part A and Part B solutions. Each calibration curve contained 18-points and were compared to a calibration curve created through the variable volume loop system and through the combustion of NIST SRM anions mentioned in **Section 2.2.**

Expected calibrant values are reported in **Tables 17-19** below with their expanded uncertainties. Coverage factor $k = 2$ was used in calculating the uncertainty.

Table 17. Mass fractions of compounds and total fluorine mass fraction in solutions containing RM 8446 Part A.

	Calibration Level					
Compound Mass Fraction (mg/kg)	**1**	**2**	**3**	**4**	**5**	**6**
PFHxA	8.51 ± 0.20	4.32 ± 0.10	1.73 ± 0.04	0.861 ± 0.02	0.436 ± 0.01	0.174 ± 0.004
PFHpA	11.15 ± 1.06	5.66 ± 0.54	2.27 ± 0.22	1.128 ± 0.107	0.571 ± 0.054	0.228 ± 0.022
PFOA	8.16 ± 0.33	4.14 ± 0.17	1.66 ± 0.07	0.825 ± 0.033	0.418 ± 0.017	0.166 ± 0.007
PFNA	9.48 ± 0.21	4.81 ± 0.11	1.93 ± 0.04	0.96 ± 0.021	0.486 ± 0.011	0.194 ± 0.004
PFDA	8.82 ± 0.61	4.48 ± 0.31	1.80 ± 0.12	0.893 ± 0.061	0.452 ± 0.031	0.18 ± 0.012
PFUnA	9.61 ± 0.99	4.88 ± 0.50	1.96 ± 0.20	0.972 ± 0.101	0.492 ± 0.051	0.196 ± 0.02
PFDoA	9.16 ± 1.08	4.65 ± 0.55	1.87 ± 0.22	0.927 ± 0.109	0.469 ± 0.055	0.187 ± 0.022
PFTriA	9.73 ± 0.43	4.94 ± 0.22	1.98 ± 0.09	0.984 ± 0.044	0.499 ± 0.022	0.199 ± 0.009
PFTA	9.01 ± 0.59	4.57 ± 0.30	1.84 ± 0.12	0.912 ± 0.06	0.462 ± 0.03	0.184 ± 0.012
F Mass Fraction (mg/kg)	**83.62 ± 2.09**	**42.45 ± 1.06**	**17.04 ± 0.43**	**8.461 ± 0.211**	**4.286 ± 0.107**	**1.706 ± 0.043**

Table 18. Mass fractions of compounds and total fluorine mass fraction in solutions containing RM 8446 Part B.

	Calibration Level					
Compound Mass Fraction (mg/kg)	**1**	**2**	**3**	**4**	**5**	**6**
PFBA	24 ± 6	12 ± 3	4.6 ± 1.2	2.3 ± 0.6	1.1 ± 0.3	0.46 ± 0.12
PFPeA	39.4 ± 0.6	19.4 ± 0.3	7.66 ± 0.11	3.88 ± 0.06	1.88 ± 0.03	0.763 ± 0.011
PFOSA	43.3 ± 1.1	21.3 ± 0.5	8.4 ± 0.21	4.26 ± 0.11	2.06 ± 0.05	0.838 ± 0.021
F Mass Fraction (mg/kg)	**106 ± 6**	**52.5 ± 3.1**	**20.7 ± 1.2**	**10.5 ± 0.6**	**5.1 ± 0.3**	**2.06 ± 0.12**

Table 19. Mass fractions of certified elements in solutions containing SRM 2143 and SRM 2144.

Calibration Level	F^- Mass Fraction (mg/kg)	Cl^- Mass Fraction (mg/kg)
1	119.5 ± 0.5	121.3 ± 0.8
2	58.91 ± 0.23	59.82 ± 0.39
3	29.88 ± 0.12	30.34 ± 0.20
4	23.63 ± 0.09	24.00 ± 0.15
5	11.64 ± 0.05	11.82 ± 0.08
6	5.750 ± 0.023	5.840 ± 0.038
7	2.417 ± 0.010	2.454 ± 0.016

2.7. Fluorine Recovery of PFAS and Other Organofluorines

Third-party neat analytical standards and NIST SRM 2143 dissolved in a water/methanol mixture mentioned in **Section 2.6** were combusted to study the fluorine recoveries of various PFAS compounds.

2.8. Effects of Cations on Fluoride Measurements

The impact of cations on fluorine determinations was studied by spiking NIST SRM 3183 (Fluoride Anion) with various amounts of either NIST SRM 3129a (Lithium Standard Solution) or SRM 3109a (Calcium Standard Solution). **Tables 20 and 21** contains the concentrations of fluoride, lithium, and calcium in each solution, given in terms of mass fractions.

Table 20. Mass fractions of lithium cation and fluoride anions in each solution (k=2).

Solution	Li^+ Mass Fraction (mg/kg)	F^- Mass Fraction (mg/kg)	Li^+:F^- Ratio
LiF 1	1057 ± 3	98.20 ± 0.31	10.76 ± 0.05
LiF 2	107.2 ± 0.4	98.92 ± 0.31	$1.084 \pm 5 \times 10^{-3}$
LiF 3	10.64 ± 0.05	98.17 ± 0.31	$0.1084 \pm 6 \times 10^{-4}$
LiF 4	$1.065 \pm 5 \times 10^{-3}$	98.68 ± 0.31	$0.01079 \pm 6 \times 10^{-5}$
LiF 5	$0.1039 \pm 5 \times 10^{-4}$	99.27 ± 0.31	$1.047 \times 10^{-3} \pm 6 \times 10^{-6}$
LiF 6	$0.0103 \pm 6 \times 10^{-5}$	98.76 ± 0.31	$104.3 \times 10^{-6} \pm 7 \times 10^{-7}$
LiF 7	-	99.89 ± 0.31	0

Table 21. Mass fractions of calcium cation and fluoride anions in each solution (k=2).

Solution	Ca^{2+} Mass Fraction (mg/kg)	F^- Mass Fraction (mg/kg)	Ca^{2+}:F^- Ratio
CaF 1	1052.3 ± 2.4	98.70 ± 0.31	10.66 ± 0.04
CaF 2	104.9 ± 0.3	99.64 ± 0.31	$1.053 \pm 5 \times 10^{-3}$
CaF 3	10.46 ± 0.04	99.86 ± 0.31	$0.1047 \pm 5 \times 10^{-4}$
CaF 4	$1.033 \pm 4 \times 10^{-3}$	99.12 ± 0.31	$0.01042 \pm 6 \times 10^{-5}$
CaF 5	$0.1017 \pm 5 \times 10^{-4}$	99.38 ± 0.31	$1.023 \times 10^{-3} \pm 6 \times 10^{-6}$
CaF 6	$9.88 \times 10^{-3} \pm 5 \times 10^{-5}$	98.20 ± 0.31	$100.6 \times 10^{-6} \pm 6 \times 10^{-7}$
CaF 7	-	98.81 ± 0.31	0

2.9. Concurrent Sulfur Determinations

Initially, 500 mg/L H_2O_2 dissolved in UPW was used for the absorption solution, but poor sulfur recovery was observed. Excellent sulfur recovery was observed at a lower concentration of 100 mg/L H_2O_2. Any measurements reporting sulfur were measured with an absorber solution concentration of 100 mg/L H_2O_2. All H_2O_2 solutions were used within 7 days of its preparation. To show the effectiveness, NIST SRM 1646a was analyzed for its sulfur content. Within the same analytical run, NIST SRM 1635a was analyzed for its fluorine content. Conversions from sulfate mass fraction to sulfur mass fraction was done by multiplying the sulfate mass fraction by 0.3337.

3. Measurement Uncertainties

3.1. Volumetric Measurements

Motorized burettes of volumes 2 mL, 5 mL, and 10 mL were used to dispense solutions throughout the operation of the CIC instrument. All burettes were certified by Metrohm to conform to ISO 8655-3 [56]. The maximum permissible random error was taken to be the uncertainty for the volumetric measurements.

ISO 8655-3 uses **Equation 19** to calculate the maximum permissible error for the selected volume e_{V_S}. V_{Nom} is the nominal volume of the burette and V_s is the selected volume. $e_{V_{Nom}}$ is the maximum permissible error for the nominal volume.

$$e_{V_S} = \frac{V_{Nom}}{V_S} \times e_{V_{Nom}} \tag{19}$$

Combined uncertainty was calculated for each volumetric measurement by first assuming that the uncertainties corresponding to each type of error follows a rectangular distribution and that one-half of the width corresponds to e_{V_S} (**Equation 20**).

$$u_{V_S} = \sqrt{\frac{e_{V_S}^2}{3}} = \sqrt{\frac{\left(\frac{V_{Nom}}{V_S} \times e_{V_{Nom}}\right)^2}{3}} = \frac{V_{Nom} e_{V_{Nom}}}{\sqrt{3} V_S} \tag{20}$$

Then, the two uncertainties were combined in quadrature. e_c is the combined permissible error of which maximum permissible systematic errors and random errors were added in quadrature (**Equation 21**).

$$u_c = \sqrt{u_{sys}^2 + u_{ran}^2} = \frac{V_{Nom}}{\sqrt{3} V_S} \sqrt{e_{V_{Nom,sys}}^2 + e_{V_{Nom,ran}}^2} = \frac{V_{Nom}}{\sqrt{3} V_S} e_c \tag{21}$$

Expanded uncertainties were calculated using a coverage factor k of 2 (**Equation 22**).

$$U = k u_c = \frac{2 V_{Nom}}{\sqrt{3} V_S} e_c \tag{22}$$

3.1.1. 2 mL Motorized Burettes

The 2 mL burette was used to dispense regenerant into the suppressor module, which is rinsed with 1.2 mL of 0.5 M H_2SO_4 solution every 9.0 minutes (**Table 22**).

Table 22. Maximum permissible errors allowed for nominal volumes between 1 mL to 2 mL.

Error Component	Value (%)
Maximum permissible systematic error	0.50
Maximum permissible random error	0.10
Combined permissible error	**0.51**

3.1.2. 5 mL Motorized Burettes

The 5 mL burette was used to dispense ultrapure water, in addition to transporting absorption solution between the absorber module and the ion chromatograph. For volumes higher than 10 % of the nominal volume (i.e. $5 * 0.1 = 0.5$ mL), random and systematic uncertainties were obtained by using calculations set forth in ISO 8655-3 (**Table 23**).

Table 23. Maximum permissible errors allowed for nominal volumes between 2 mL to 5 mL.

Error Component	Value (%)
Maximum permissible systematic error	0.30
Maximum permissible random error	0.10
Combined permissible error	**0.32**

3.1.3. 10 mL Motorized Burettes

The 10 mL burette was used to dispense absorber solution into the outlet of the combustion oven (**Table 24**).

Table 24. Maximum permissible errors allowed for nominal volumes between 5 mL to 25 mL.

Error Component	Value (%)
Maximum permissible systematic error	0.20
Maximum permissible random error	0.070
Combined permissible error	**0.21**

3.1.4. Estimated Uncertainties for IC Injection Volumes

Although the 5 mL motorized burette controls the IC injection volume, ISO 8655-3 does not cover uncertainty calculations for volumes below 10 % of the nominal volume and there was no deviation data in the product specifications. In addition, it is difficult to replicate the conditions in which the system operates in, as the fluid lines are always under high pressure. Therefore, the volumes are estimates made from the calibration curve equations (described in **Section 0**).

3.2. Conductivity Measurements and Peak Area Integrations

Conductivity ($\sigma_{measured}$) was measured using a conductivity meter (Metrohm 2.850.9010 IC Conductivity Detector). Technical specifications of the conductivity meter are presented in **Table 25** and calibration values for the conductivity meter are presented in **Table 26**. The unit for electrical conductance is siemens (S) and is defined, in SI base units, as $m^{-2} \cdot kg^{-1} \cdot s^3 \cdot A^2$.

Table 25. Technical specifications of the conductivity meter.

Parameter	Provided Value
Linearity Deviation	$\begin{cases} < 0.1\ \% \ (> 16\ \mu S \times cm^{-1}) \\ < 1\ \% \ (\leq 16\ \mu S \times cm^{-1}) \end{cases}$
Measuring Range	$0\ \mu S \times cm^{-1}$ to $15{,}000\ \mu S \times cm^{-1}$
Sampling Rate	10 Hz
Conductance Noise	$< 0.1\ nS$ (at $1\ \mu S \times cm^{-1}$)
Resolution	$0.0047\ nS \times cm^{-1}$
Drift	$< 0.2\ \mu S \times cm^{-1} \times h^{-1}$
Baseline Noise	$< 0.2\ nS \times cm^{-1}$

Table 26. Conductivity meter calibration parameters.

Parameter	Set Value
Cell Constant	$18.0\ cm^{-1}$

Ideally, the uncertainties of each conductivity measurement for a given peak integration would be combined to calculate peak area uncertainty u_A. Using the instrument software, preset variables such as peak area, peak retention time, and peak height can be exported; however, individual conductivity values cannot be exported. As such, an indirect determination of peak area uncertainty was determined by taking the standard deviation of fluoride peak areas of all CCVs for a given analytical run originating from the same calibration solution. Fluoride was chosen as it has the highest sensitivity out of all anions in this study. Peak area integration was performed using the software's algorithm and no manual adjustments were performed.

3.3. Mass and Mass Fraction Measurements

3.3.1. Masses Weighed to 5 Decimal Points

In most cases, a 5-decimal analytical scale was used to gravimetrically prepare solutions. **Table 27** displays the uncertainty components provided by the manufacturer.

Table 27. 5-decimal analytical scale uncertainty values provided by manufacturer.

Uncertainty Component	Value
$u_{linearity}$	0.06 mg
$u_{readability}$	0.01 mg
$u_{eccentricity}$	0.1 mg
$u_{repeatability}$	0.08 mg

Assuming a rectangular distribution for all values, the typical linearity deviation, readability, eccentricity, and repeatability values reported in the tool specifications were used to calculate a standard uncertainty. All masses reported required two separate mass measurements, once to tare and once to measure gross weight. Assuming those two events were independent of each other, the uncertainty was propagated to include both measurements. Coverage factor $k = 2$ was used to expand the uncertainty to meet a 95 % level of confidence unless noted otherwise (**Equation 23**). U is defined as the combined and expanded uncertainty for masses weighed using this scale.

$$U = 2 \times \sqrt{2 \times \left(\frac{u_{linearity}^2 + u_{readability}^2 + u_{eccentricity}^2 + u_{repeatability}^2}{3} \right)} = 0.00023 \text{ g} \quad (23)$$

3.3.2. Masses Weighed to 2 Decimal Points.

The 2 mg/kg anion external calibration solutions, eluent solutions, and absorption solutions were prepared gravimetrically using a 2 decimal analytical scale. Like the 5-decimal analytical scale, a rectangular distribution was assumed for all values reported by the manufacturer and the uncertainty was expanded by a coverage factor *k* equal to 2 unless noted otherwise (**Table 28, Equation 24**). U is defined as the combined and expanded uncertainty for masses weighed using this scale.

Table 28. Uncertainty components of masses weighed to 2 decimal points.

Uncertainty Component	Value
$u_{linearity}$	0.01 g
$u_{readability}$	0.01 g
$u_{repeatability}$	0.01 g

$$U = 2 \times \sqrt{2 \times \left(\frac{u_{linearity}^2 + u_{readability}^2 + u_{repeatability}^2}{3} \right)} = 0.03 \text{ g} \quad (24)$$

3.3.3. On-column Analyte Mass

The on-column analyte mass on column refers to the mass of halides that make it onto the analytical column, which is then measured using the conductivity sensor. This variable is calculated using a calibration curve that relates the peak area to the amount of mass injected into the IC. Note that the amount of analyte that make it onto the analytical column is likely less than the injected amount and cannot be easily characterized. For example, there may be absorption of the analyte into the tubing lining or semi-permanent adsorption of analytes to the concentrator column. In this report, we assumed that such phenomena were accounted for through the creation of a calibration curve for each analytical run.

The instrument response to analyte mass is modeled through **Equation 25** (linear fit) or **Equation 26** (quadratic fit).

$$m_{analyte} = \frac{A - a_0}{a_1} \tag{25}$$

$$m_{analyte} = \frac{-a_1 \pm \sqrt{a_1^2 - 4a_2(a_0 - A)}}{2a_2} \tag{26}$$

In either case, the estimated on-column analyte mass uncertainty has components arising from the fitness of the calibration curve. $r(a_i, a_j)$ is the correlation coefficient for coefficients a_i and a_j. The equations used to calculate mass uncertainty, and their derivation can be found in **Appendix B.** Uncertainty of the model parameters were taken to be the standard errors resulting from the fit.

This calculation must be done for each calibration curve fit. The code in **Appendix C** was used to compute the on-column analyte mass and the associated uncertainty.

3.3.4. Mass Fractions and Concentrations

Uncertainties regarding mass fractions and concentrations for this report were calculated using the method stated below. In general, a dilution factor was calculated, then multiplied to the corresponding analyte mass fraction to determine the new mass fraction.

Two cases were considered – one where the initial solution was diluted with a solvent and another where multiple solutions were combined into one. In both cases, all measurements were assumed to be independent from each other.

3.3.4.1. Dilution of a Solution Containing Multiple Analytes

As an example, consider a dilution created from solution A containing n number of analytes (**Table 29**).

Table 29. Example dilution of a solution containing n analytes.

Component	A	Solvent
Analyte Mass Fraction ($\boldsymbol{w_i}$)	$w_1, w_2, \dots, w_n$	-

Mass added	m_1	m_2
Dilution Factor ($\boldsymbol{X}$)	$\frac{m_1}{m_1+m_2}$	-

In this case, the dilution factor X is equal to $\frac{m_1}{m_1+m_2}$, regardless of analyte. The uncertainty of the dilution factor u_X was then propagated (**Equation 27**).

$$u_X = \sqrt{\left(u_{m_1} \times \frac{\partial X}{\partial m_1}\right)^2 + \left(u_{m_2} \times \frac{\partial X}{\partial m_2}\right)^2} = \sqrt{\left(u_{m_1} \times \frac{m_2}{(m_1+m_2)^2}\right)^2 + \left(u_{m_2} \times \frac{-m_1}{(m_1+m_2)^2}\right)^2} \quad (27)$$

If u_{m_1} and u_{m_2} are equal, the equation above is simplified further (**Equation 28**).

$$u_X = \sqrt{\left(\frac{u_m}{(m_1+m_2)^2}\right)^2 \times (m_1^2+m_2^2)} = \frac{\sqrt{m_1^2+m_2^2}}{(m_1+m_2)^2} \times u_m \quad (28)$$

The new mass fraction of the i-th analyte w_{new_i} is equal to $X * w_i$. The uncertainty of the new mass fraction $u_{w_{new,i}}$ is determined by propagation (**Equation 29**).

$$u_{w_{new_i}} = \sqrt{\left(u_X \times \frac{\partial w_{new_i}}{\partial X}\right)^2 + \left(u_{c_i} \times \frac{\partial w_{new_i}}{\partial w_i}\right)^2} = \sqrt{(u_X \times w_i)^2 + \left(u_{w_i} \times X\right)^2} \quad (29)$$

3.3.4.2. Solution Created from Addition of Solutions

For solutions created by the addition of multiple other solutions, the dilution factor for each component of the final solution was first calculated. Then, the uncertainty of the dilution factor was calculated.

As an example, consider a solution created by the addition of five separate solutions, each containing one analyte (**Table 30**).

Table 30. Table containing five hypothetical solutions and their associated experimental parameters.

Solution	**A**	**B**	**C**	**D**	**E**
Original Mass Fraction	w_1	w_2	w_3	w_4	w_5
Mass Combusted	m_1	m_2	m_3	m_4	m_5
Dilution Factor ($\boldsymbol{X_i}$)	$\frac{m_1}{\sum_{i=1}^{5} m_i}$	$\frac{m_2}{\sum_{i=1}^{5} m_i}$	$\frac{m_3}{\sum_{i=1}^{5} m_i}$	$\frac{m_4}{\sum_{i=1}^{5} m_i}$	$\frac{m_5}{\sum_{i=1}^{5} m_i}$

The dilution factor of the i-th component X_i is equal to $\frac{m_i}{\sum_{i=1}^{5} m_i}$. The uncertainty associated with this dilution u_{X_i} is calculated by propagation (**Equation 31**).

$$u_{X_i} = \sqrt{\sum_{n=1}^{5} \left(u_{m_n} \times \frac{\partial X}{\partial m_n} \right)^2}$$

$$= \sqrt{\left(u_{m_i} \times \frac{(\sum_{n=1}^{5} m_n) - m_i}{(\sum_{n=1}^{5} m_n)^2} \right)^2 + \sum_{\substack{n=1 \\ n \neq i}}^{5} \left(u_{m_n} \times \frac{m_i}{(\sum_{n=1}^{5} m_n)^2} \right)^2} \quad (31)$$

If u_{m_i} is constant for all i, **Equation 31** can be simplified to **Equation 32**.

$$u_{X_i} = \sqrt{\left(u_m \times \frac{(\sum_{n=1}^{5} m_n) - m_i}{(\sum_{n=1}^{5} m_n)^2} \right)^2 + (n-1) \times \left(u_m \times \frac{m_i}{(\sum_{n=1}^{5} m_n)^2} \right)^2}$$

$$= \frac{\sqrt{(\sum_{n=1}^{5} (m_n) - m_i)^2 + (n-1) \times m_i^2}}{(\sum_{n=1}^{5} m_n)^2} \times u_m \quad (32)$$

The new mass fraction of the i-th component $w_{new,i}$ is equal to $X_i * w_i$. The uncertainty for this new mass fraction $u_{w_{new,i}}$ is determined (**Equation 33**).

$$u_{w_{new,i}} = \sqrt{\left(\frac{\partial w_{new,i}}{\partial X_i} \times u_{X_i} \right)^2 + \left(\frac{\partial w_{new,i}}{\partial w_i} \times u_{w_i} \right)^2} = \sqrt{\left(w_i \times u_{X_i} \right)^2 + \left(X_i \times u_{w_i} \right)^2} \quad (33)$$

3.3.4.3. Conversion of Concentrations to Mass Fractions

All experiments were performed in STP (20 °C, 1 atm). To convert concentration c to mass fraction w, mass concentration γ was divided by the density of the solvent ρ (**Equation 34**). Uncertainties from this conversion were ignored in this report. **Table 31** lists the values used in this report. Densities were obtained from the NIST Chemistry Webbook [57].

$$w = \frac{\gamma}{\rho} \quad (34)$$

Table 31. Densities of solvents used in this report.

Solvent	Density
Water	55.409 mol/L × 18.015 g / mol = 998.19 g/L
Methanol	24.687 mol/L × 32.042 g / mol = 791.02 g/L
Ethyl Acetate	900.3 g/L
Isooctane	691.94 g/L

3.4. Determination of Concentrations using Ion Chromatography

The mass concentration γ_{sample} , and by extension the mass fraction, of halides in liquid samples was determined by directly injecting a portion of the solution into the IC. Determination of halogen concentrations requires the knowledge of the on-column analyte mass m_{column} and IC injection volume V_{IC} (**Equation 35**).

$$\gamma_{sample} = \frac{m_{column}}{V_{IC}} \tag{35}$$

For individual concentrations, the associated uncertainties are determined using **Equation 36**.

$$u_{\gamma} = \sqrt{\left(\frac{1}{V} \times u_m\right)^2 + \left(-\frac{m}{V^2} \times u_V\right)^2} \tag{36}$$

Often, samples were injected in triplicate or more. In such cases, the reported sample concentration was the arithmetically averaged value (**Eq. 37**).

$$\gamma_{reported} = \bar{\gamma}_{sample} \tag{37}$$

For samples with n number of replicates, the uncertainty of the average mass concentration was calculated by **Equation 38**.

$$u_{\bar{\gamma}} = \frac{\sqrt{u_{\gamma_1}^2 + u_{\gamma_2}^2 + \cdots + u_{\gamma_n}^2}}{n} \tag{38}$$

3.5. Determination of Mass Fractions using Combustion Ion Chromatography

Determination of sample halogen mass fraction w_{sample} was determined similarly to mass concentration (**Equation 39**).

$$w_{sample} = \frac{m_{column}}{V_{IC}} \times \frac{V_{absorption}}{m_{combustion}} \tag{39}$$

For individual mass fractions, the associated uncertainties were calculated using **Equation 40**.

$$u_w = \sqrt{\begin{array}{l}\left(\frac{V_{absorption}}{V_{IC} \times m_{combustion}} \times u_{m_{column}}\right)^2 + \left(\frac{m_{column}}{V_{IC} \times m_{combustion}} \times u_{V_{absorption}}\right)^2 \\ + \left(\frac{m_{column} V_{absorption}}{V_{IC}^2 \times m_{combustion}} \times u_{V_{IC}}\right)^2 + \left(\frac{m_{column} \times V_{absorption}}{V_{IC} m_{combustion}^2} \times u_{m_{combustion}}\right)^2\end{array}} \tag{40}$$

Similarly to concentrations, the reported sample mass fractions were the averaged value of the triplicate samples (**Equation 41**).

$$w_{reported} = \overline{w}_{sample} \tag{41}$$

For samples with n number of replicates, the uncertainty of the averaged mass fraction was calculated with **Equation 42**.

$$u_{\overline{w}} = \frac{\sqrt{u_{w_1}^2 + u_{w_2}^2 + \cdots + u_{w_n}^2}}{n} \tag{42}$$

3.6. Determination of Recoveries

Percent recoveries R were determined by first calculating the halogen mass fraction measured by the IC/CIC $w_{Measured}$, then dividing the value by the expected halogen mass fraction of the sample $w_{Expected}$ (**Equation 43**).

$$R\ (\%) = \frac{w_{Measured}}{w_{Expected}} \times 100 \tag{43}$$

Uncertainty values of recoveries u_R were determined by propagation (**Equation 44**).

$$\begin{aligned} u_R &= \sqrt{\left(u_{w_{Measured}} \times \frac{\partial R}{\partial(w_{Measured})}\right)^2 + \left(u_{w_{Expected}} \times \frac{\partial R}{\partial(w_{Expected})}\right)^2} \\ &= \sqrt{\left(u_{w_{Measured}} \times \frac{w_{Expected}}{(w_{Expected})^2} \times 100\right)^2 + \left(u_{w_{Expected}} \times \frac{-w_{Measured}}{(w_{Expected})^2} \times 100\right)^2} \\ &= \frac{100}{(w_{Expected})^2} \times \sqrt{(u_{w_{Measured}} \times w_{Expected})^2 + (u_{w_{Expected}} \times w_{Measured})^2} \end{aligned} \tag{44}$$

In addition, relative standard deviation was reported alongside with combined uncertainties.

3.7. Determination of Mass Fraction Ratios

The ratio r between two mass fractions w_a and w_b were calculated by **Equation 45**.[5]

$$r = \frac{w_a}{w_b} \tag{45}$$

Uncertainty of r (u_r) was calculated using the following **Equation 46**.

$$\begin{aligned} u_r &= \sqrt{\left(u_{w_a} \times \frac{\partial r}{\partial w_a}\right)^2 + \left(u_{w_b} \times \frac{\partial r}{\partial w_b}\right)^2} \\ &= \sqrt{\left(u_{w_a} \times \frac{1}{w_b}\right)^2 + \left(u_{w_b} \times \frac{-w_a}{w_b^2}\right)^2} \end{aligned} \tag{46}$$

[5] Not to be confused with $r(x, y)$, the correlation coefficient of terms x and y.

3.8. Summary of Uncertainties Considered

A summary of the uncertainties considered in the determination of halogen mass fraction ratios can be found in **Table 32**.

Table 32. Uncertainty budget for the determination of mass fraction ratios according to this report.

Category	Parameter	Unit	Type	Distribution	Divisor	Degrees of Freedom
On-column Analyte Mass	Analyte Peak Area	$\frac{\mu S * min}{cm}$	A	Normal	1	(# of Cal 4 Injections) − 2
	Calibration Curve Parameter Standard Errors	Depends on model and parameter in question.[6]	A			(# of Injections in Curve) − (# of Model Parameters)
Absorber Solution Volume	Maximum permissible systematic error	mL	B	Rectangular	$\sqrt{3}$	Infinity
	Maximum permissible random error					
IC Injection Volume	Estimated Volume Uncertainty	µL	A	Normal	1	N-2 = 32
Combustion Mass	Linearity	g	B	Rectangular	$\sqrt{3}$	Infinity
	Readability					
	Eccentricity					
	Repeatability					
Average Mass Fraction Concentration	Individual Solution Concentrations	mg/L	A	Normal	1	Infinity
Mass Fraction Ratio or Recovery	Measured Value	mg/kg	A	Normal	1	Infinity
	Expected Value	mg/kg	B	Normal	1	Infinity

[6] Examples of potential units include ng, $\frac{ng^* cm}{\mu S * min}$, and $\frac{ng^* cm^2}{\mu S^2 * min^2}$.

4. Results

4.1. Instrument Response and Characterization of Partial Loop Injection System

Except for fluoride, a linear instrument response model provided the best fit for the halide and sulfate CIC data. A quadratic response model was best for fluoride in the targeted mass range (approximately 2 ng to 400 ng). This is observed (**Figure 6**) where there is a maximum sensitivity at approximately 37.66 µL and a subsequent decrease in sensitivity with increasing injection volume set point (i.e., increasing on-column fluoride mass). For a linear model, the global maximum should exist at the end of the mass range. Sensitivity plots for other analytes can be seen in **Appendix D.1**.

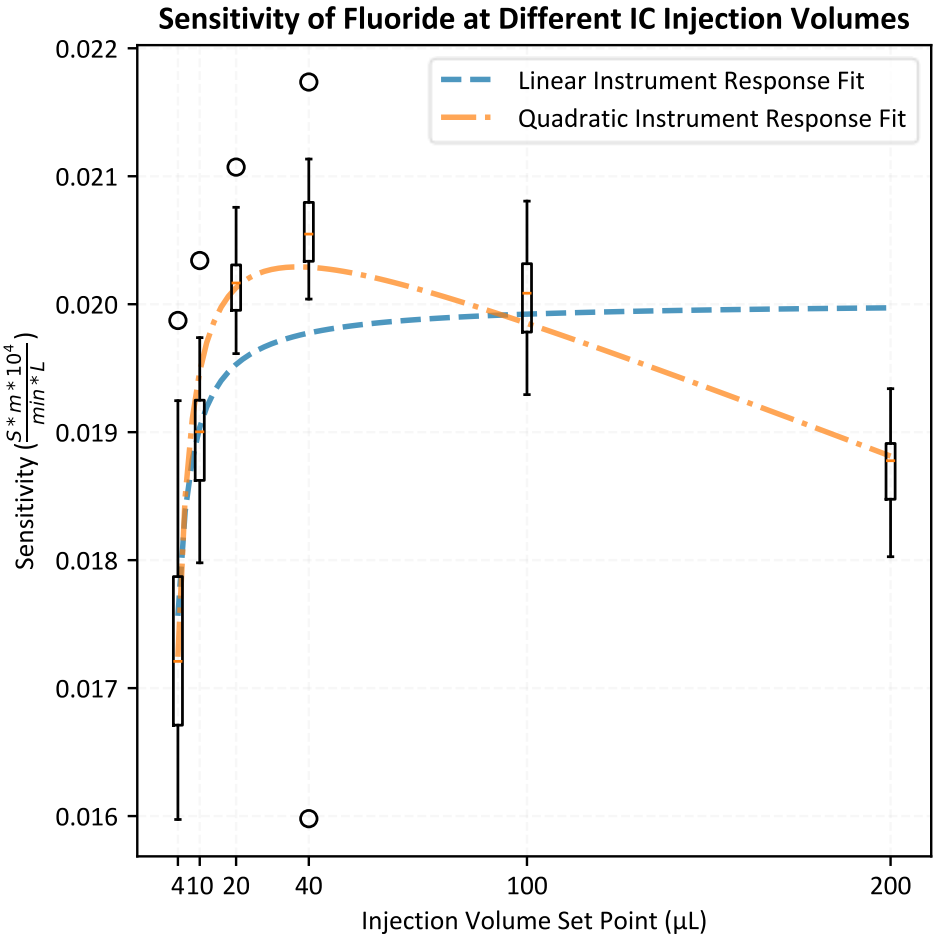

Figure 6. Fluoride sensitivities at different IC injection volume set points. Circles represent outliers, orange lines represent the median, boxes represent the first to third quartile of the data, and whiskers represent the farthest data point lying within the 1.5x the inter-quartile range. Outliers are defined as any data points that fall outside of the 1.5x the inter-quartile range.

Using the fluoride calibration data, estimated IC injection volumes and their associated standard deviations were calculated and plotted (**Figure 7**) and tabulated (**Table 33**). Fluoride was chosen as it has the highest sensitivity out of all the analytes. Standard deviations from each IC injection

volume set point presented in **Table 33** was used to calculate uncertainties for subsequent measurements in this report.

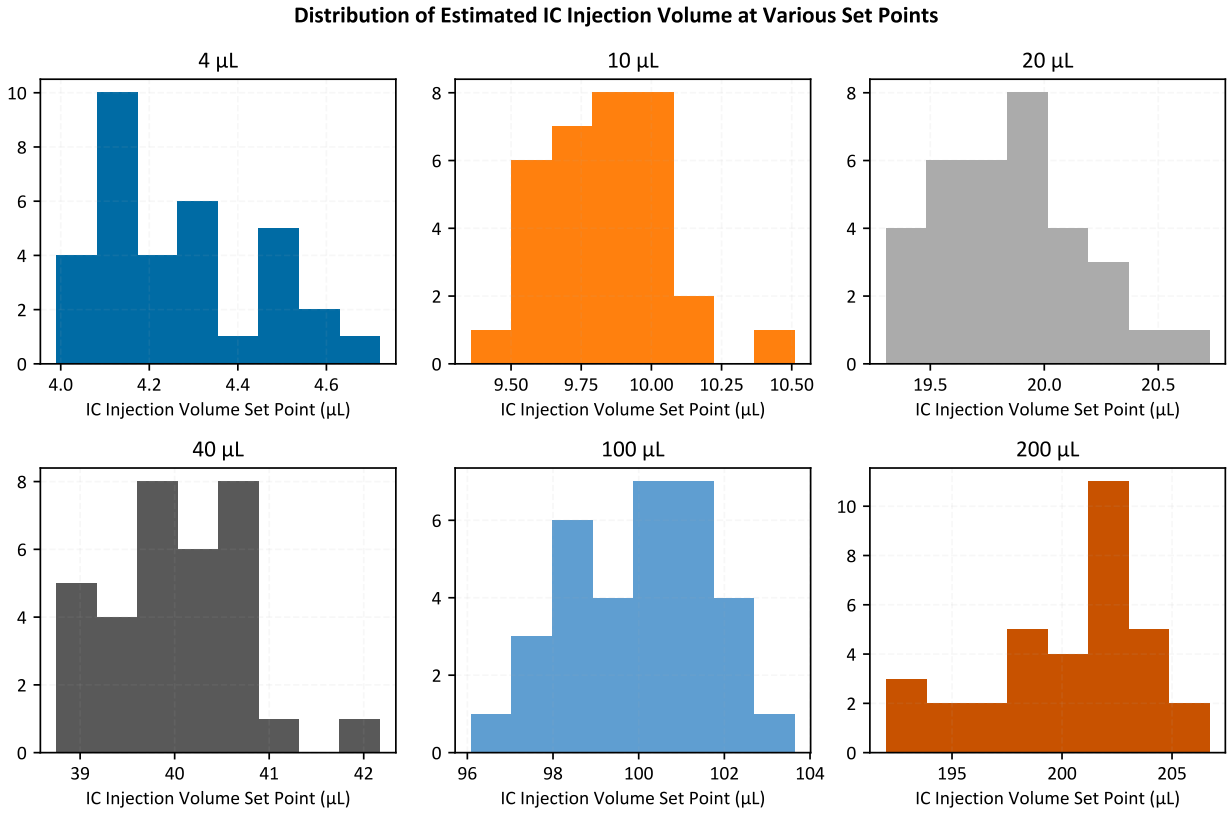

Figure 7. Estimated IC injection volumes using fluoride calibration data (quadratic fit).

Table 33. IC injection volume and associated uncertainties estimated using fluoride calibration data (quadratic fit).

IC Injection Volume Set Point (µL)	Estimated IC Injection Volume (µL)	Standard Deviation (µL)
4	4.2781	0.2003
10	9.8453	0.2433
20	19.867	0.359
40	39.960	0.746
100	100.03	1.58
200	200.08	3.81

4.2. Creation of Organofluorine and Organochlorine Calibration Curves

To determine the accuracy and reliability of using organic halogenated compounds for calibration purposes, organic halogenated compounds found in RM 8446, SRM 2143, SRM 2144 were analyzed via CIC compared to inorganic compounds found in SRM 3182, 3183, 3184 analyzed via IC/CIC. Direct injection in this section refers to ERA Custom Anions Mix 3 standard solution injected directly into the IC. Organobromine calibration curves could not be created as there currently are no NIST high-purity SRMs containing organic bromine compounds. **Tables 34-39** list the CIC/IC parameters for each solution.

Table 34. CIC parameters for RM 8446 Part A.

Calibration Level	IC Injection Volume (µL)	Solution Mass Fraction (mg/kg)	Solution Combusted (mg)	Estimated F^- Mass Injected (ng)
1	200 ± 7.62	83.62 ± 2.09	69.55 ± 0.13	197.29 ± 0.38
2	200 ± 7.62	42.45 ± 1.06	70.13 ± 0.13	101.12 ± 0.19
3	200 ± 7.62	17.04 ± 0.43	66.74 ± 0.13	38.69 ± 0.08
4	200 ± 7.62	8.461 ± 0.211	75.08 ± 0.13	21.46 ± 0.04
5	200 ± 7.62	4.286 ± 0.107	67.97 ± 0.13	9.84 ± 0.02
6	200 ± 7.62	1.706 ± 0.043	75.59 ± 0.13	4.36 ± 0.01

Table 35. CIC parameters for RM 8446 Part B.

Calibration Level	IC Injection Volume (µL)	Solution Mass Fraction (mg/kg)	Solution Combusted (mg)	Estimated Cl^- Mass Injected (ng)
1	200 ± 7.62	106 ± 6	63.36 ± 0.13	228.68 ± 0.92
2	200 ± 7.62	52.5 ± 3.1	66.5 ± 0.13	118.83 ± 0.48
3	200 ± 7.62	20.7 ± 1.2	68.78 ± 0.13	48.22 ± 0.18
4	200 ± 7.62	10.5 ± 0.6	80.02 ± 0.13	28.47 ± 0.09
5	200 ± 7.62	5.1 ± 0.3	71.75 ± 0.13	12.36 ± 0.05
6	200 ± 7.62	2.06 ± 0.12	71.09 ± 0.13	4.96 ± 0.02

Table 36. CIC parameters for solutions containing both SRM 2143, 2144.

Calibration Level	IC Injection Volume (µL)	Solution Mass Fraction (mg/kg)		Solution Combusted (mg)	Estimated Mass Injected (ng)	
		F^-	Cl^-		F^-	Cl^-
1	200 ± 7.62	119.5 ± 0.5	121.3 ± 0.8	94.61 ± 0.13	390.79 ± 0.28	396.67 ± 0.29
2	200 ± 7.62	58.91 ± 0.23	59.82 ± 0.39	95.24 ± 0.13	193.94 ± 0.13	196.93 ± 0.14
3	200 ± 7.62	29.88 ± 0.12	30.34 ± 0.20	95.74 ± 0.13	98.88 ± 0.07	100.4 ± 0.07
4	200 ± 7.62	23.63 ± 0.09	24.00 ± 0.15	96 ± 0.13	78.41 ± 0.05	79.64 ± 0.06
5	200 ± 7.62	11.64 ± 0.05	11.82 ± 0.08	92.45 ± 0.13	37.2 ± 0.03	37.77 ± 0.03
6	200 ± 7.62	5.750 ± 0.023	5.840 ± 0.038	96.61 ± 0.13	19.2 ± 0.01	19.5 ± 0.01
7	200 ± 7.62	2.417 ± 0.010	2.454 ± 0.016	96.98 ± 0.13	8.1 ± 0.01	8.23 ± 0.01

Table 37. CIC parameters for solution containing SRM 3182, 3183, 3184.

Calibration Level	IC Injection Volume (µL)	Solution Mass Fraction (mg/kg)	Solution Combusted (mg)
		F^-, Cl^-, Br^-	
1	200 ± 7.62	99.20 ± 0.05	100.52 ± 0.13
2	100 ± 3.16	99.20 ± 0.05	99.73 ± 0.13
3	50 ± 1.77	99.20 ± 0.05	100.43 ± 0.13
4	25 ± 0.96	99.20 ± 0.05	97.42 ± 0.13
5	12.5 ± 0.54	99.20 ± 0.05	100.66 ± 0.13
6	6.25 ± 0.43	99.20 ± 0.05	100.34 ± 0.13
7	4 ± 0.4	99.20 ± 0.05	100.33 ± 0.13

Table 38. Additional CIC parameters for solution containing SRM 3182, 3183, 3184.

Calibration Level	Estimated Mass Injected (ng)		
	F^-	Cl^-	Br^-
1	344.67 ± 0.22	346.27 ± 0.22	346.06 ± 0.22
2	170.99 ± 0.09	171.78 ± 0.09	171.68 ± 0.09
3	86.1 ± 0.05	86.49 ± 0.05	86.44 ± 0.05
4	41.76 ± 0.03	41.95 ± 0.03	41.93 ± 0.03
5	21.57 ± 0.02	21.67 ± 0.02	21.66 ± 0.02
6	10.75 ± 0.01	10.8 ± 0.01	10.79 ± 0.01
7	6.88 ± 0.01	6.91 ± 0.01	6.91 ± 0.01

Table 39. IC parameters for ERA Custom Mix 3.

Calibration Level	IC Injection Volume (µL)	Solution Mass Fraction (mg/kg)	Estimated Mass Injected (ng)
		F^-, Cl^-, Br^-	F^-, Cl^-, Br^-
1	200 ± 7.62	2.05 ± 0.02	410.74 ± 5.08
2	200 ± 7.62	1.02 ± 0.01	204.37 ± 2.53
3	200 ± 7.62	$0.42 \pm 4 \times 10^{-3}$	84.15 ± 1.03
4	200 ± 7.62	$0.213 \pm 2 \times 10^{-3}$	42.68 ± 0.52
5	200 ± 7.62	$0.103 \pm 1 \times 10^{-3}$	20.64 ± 0.25
6	200 ± 7.62	$0.0408 \pm 4 \times 10^{-4}$	8.17 ± 0.1

For fluorine, all curves created using CIC showed steeper slopes than the direct injection curves as seen in **Figure 8**. Dotted lines indicate extrapolation to the highest injected fluorine mass. This could be attributed to background fluorine, though it is unclear why curves created from RM 8446 have much higher slopes.

For chlorine and bromine, all curves created using CIC showed smaller slopes than the direct injection curves as seen in **Figures 9 and 10**. Dotted lines indicate extrapolation to the highest injected chlorine/bromine mass. This is likely due to the losses during the combustion process. It may be worth noting that the organochlorine curve has the smallest slope. Additional information regarding the fitting can be found in **Appendix D.2**.

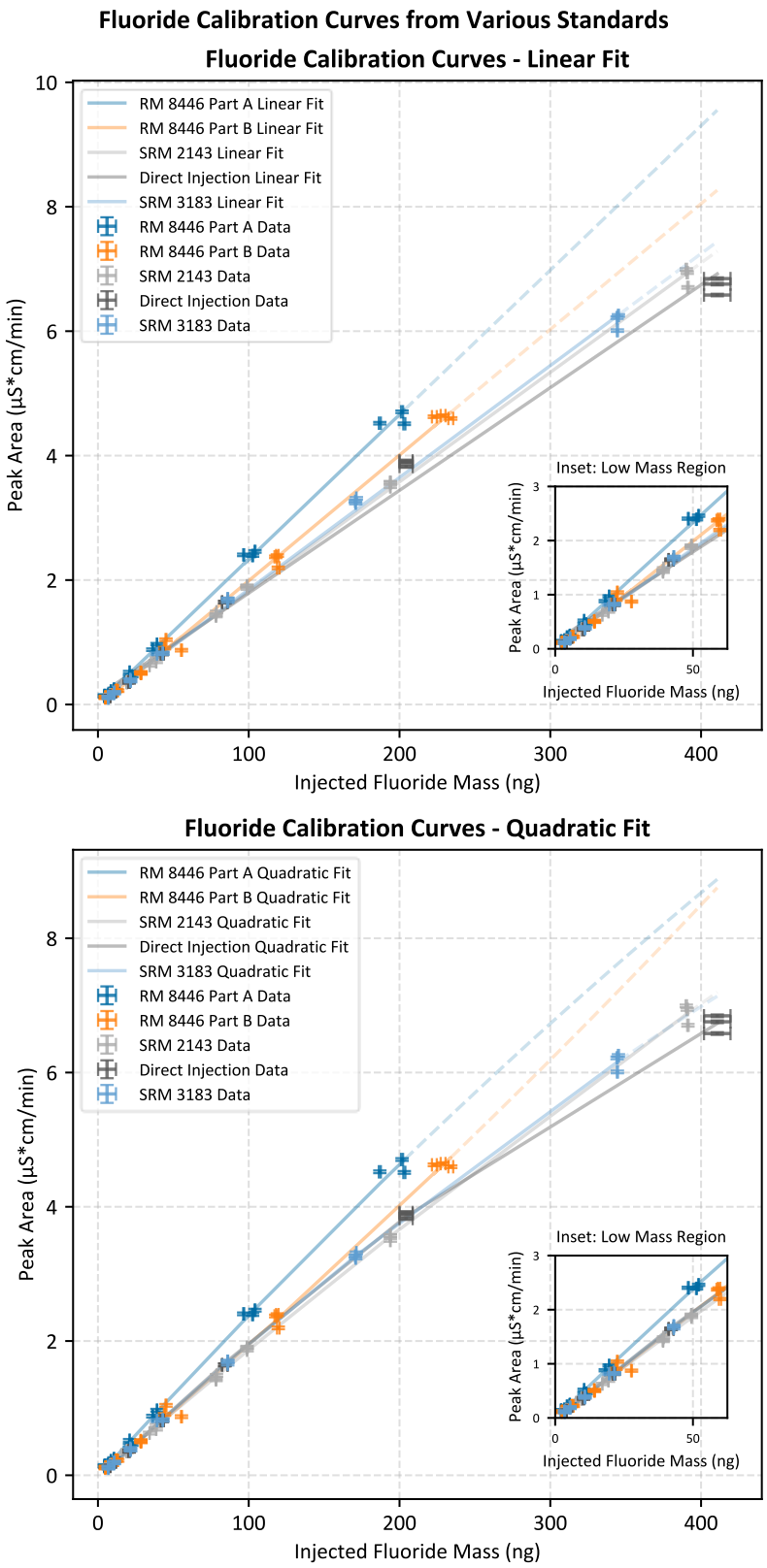

Figure 8. Fluoride calibration curves created using various standards. Dotted lines represent data extrapolation to the highest injected fluoride mass.

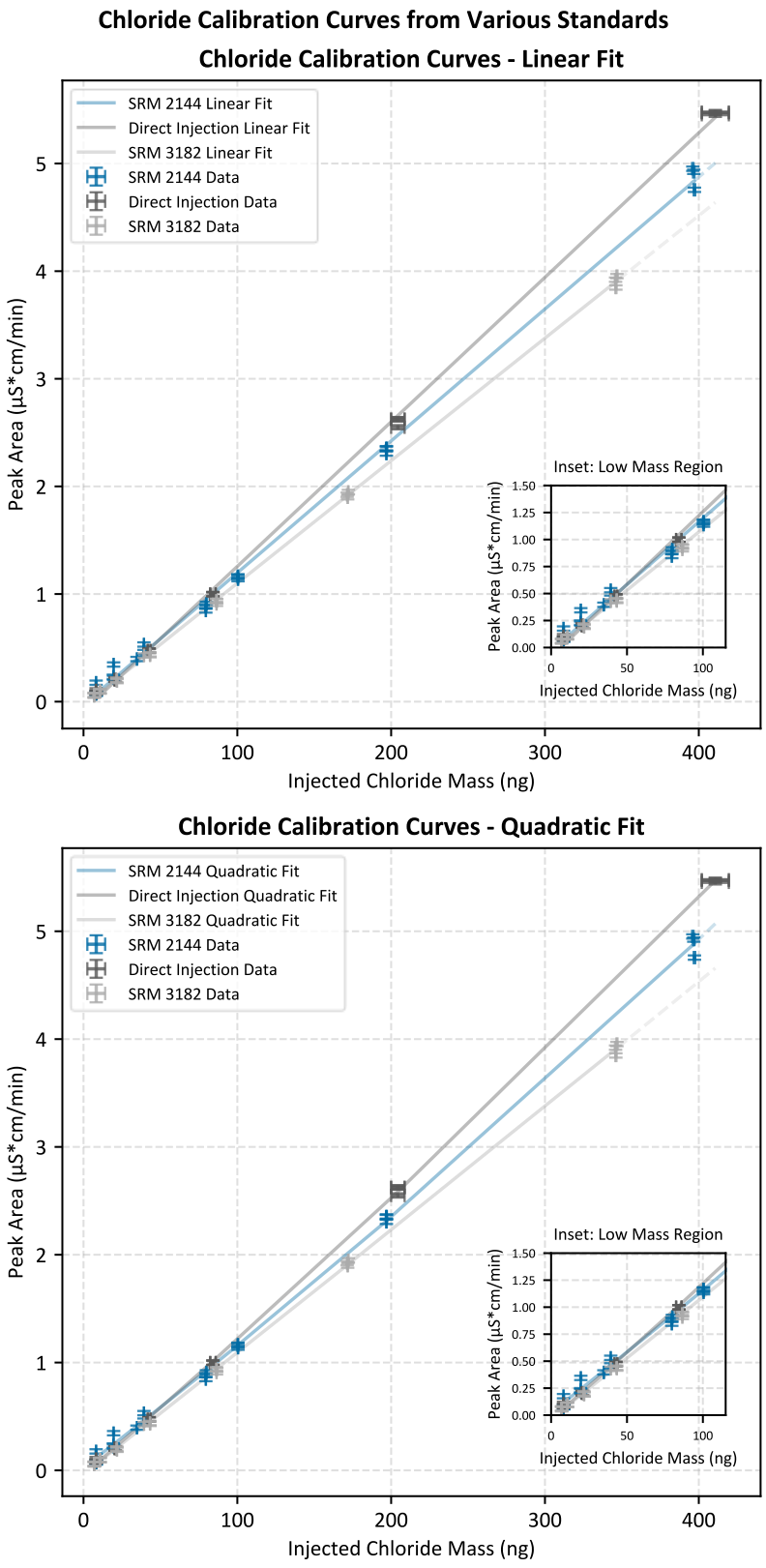

Figure 9. Chloride calibration curves created using various standards. Dotted lines represent data extrapolation to the highest injected chloride mass.

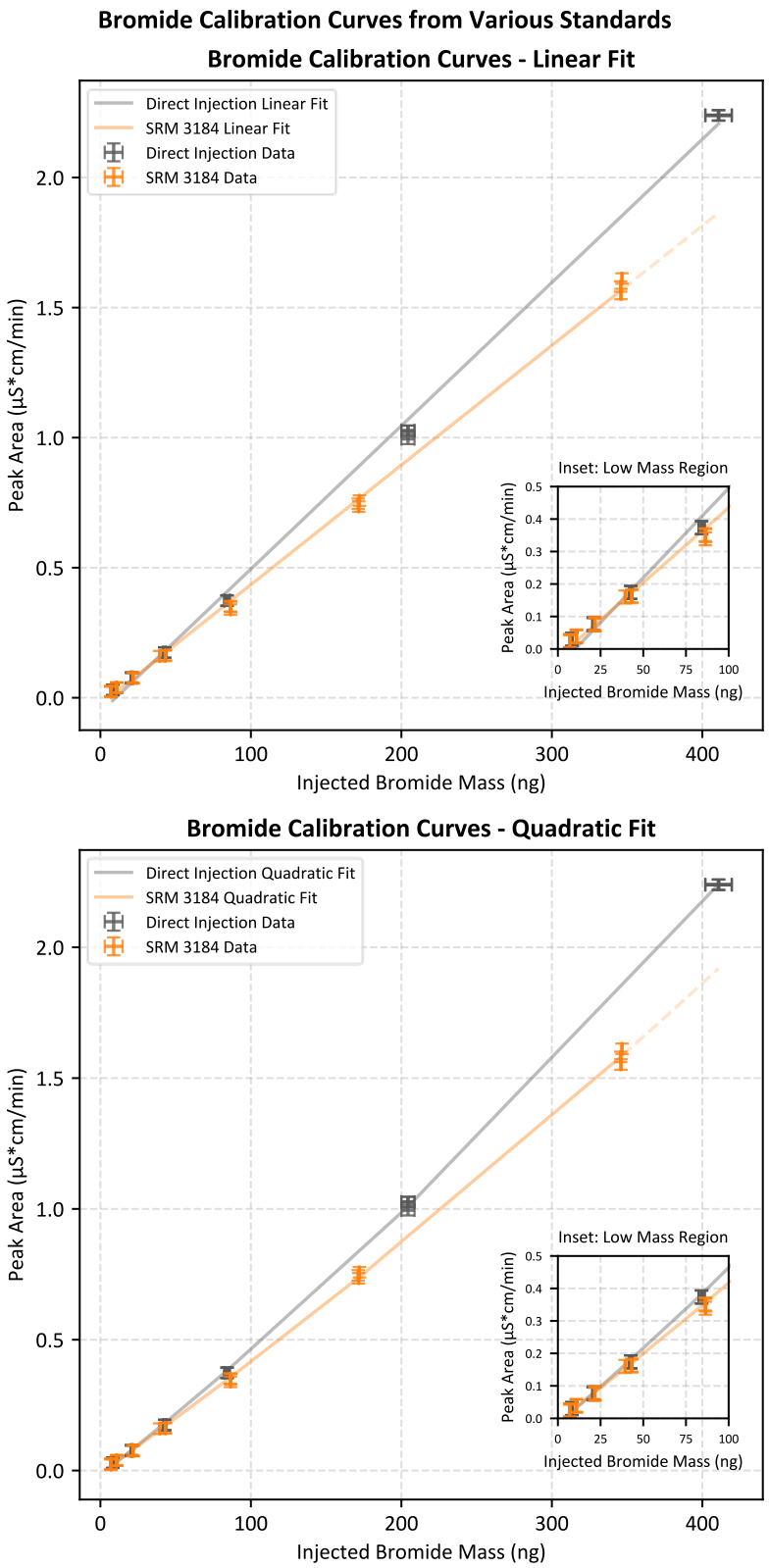

Figure 10. Bromide calibration curves created using various standards. Dotted lines represent data extrapolation to the highest injected bromide mass.

4.3. Fluoride Recovery of PFAS and Other Organofluorines

Tables 40 and 41 show the measured fluoride mass fractions of NIST RM 8446 Parts A and B without any blank correction. Overall, the measured fluoride mass fractions without any blank correction are higher than the expected values (**Tables 17 and 18**), except for RM 8446 Part B calibration levels 1 through 4.

Table 40. RM 8446 Part A fluoride mass fraction results (no blank correction).

Calibration Level	Sample F^- Mass Fraction (mg/kg, k=1)	Standard Deviation (mg/kg)	Recovery (%, k=1)
1	95.89 ± 0.65	3.39	114.7 ± 1.6
2	48.73 ± 0.37	1.65	114.8 ± 1.7
3	19.29 ± 0.23	1.61	113.2 ± 2.0
4	9.529 ± 0.183	0.999	112.6 ± 2.6
5	5.692 ± 0.195	0.439	132.8 ± 4.9
6	3.372 ± 0.172	0.224	197.7 ± 10.4

Table 41. RM 8446 Part B fluoride mass fraction results (no blank correction).

Calibration Level	Sample F^- Mass Fraction (mg/kg, k=1)	Standard Deviation (mg/kg)	Recovery (%, k=1)
1	105.9 ± 0.7	2.5	99.87 ± 2.91
2	49.11 ± 0.38	2.32	93.54 ± 2.85
3	19.86 ± 0.23	3.83	95.94 ± 2.99
4	9.428 ± 0.172	0.203	89.79 ± 3.04
5	5.194 ± 0.194	0.298	101.8 ± 4.7
6	3.218 ± 0.183	0.117	156.2 ± 10.0

When fluoride mass fractions are corrected with methanol blanks (**Table 42**), most measured values were below the expected value, particularly at lower calibration levels (**Tables 43 and 44**). We observed more calibration levels out of the acceptable recovery range of 80 % to 120 % when compared to the non-corrected recoveries as seen in **Figure 11**.

Table 42. Averaged apparent fluoride concentration of adsorption solution of methanol blanks (N=4).

Apparent F^- Concentration (mg/µL)	Standard Deviation (mg/µL)	IC Injection Volume Set Point (µL)
2.715×10^{-8}	3.372×10^{-9}	200

Table 43. RM 8446 Part A fluoride mass fraction results (with blank correction).

Calibration Level	Sample F^- Mass Fraction (mg/kg)	Standard Deviation (mg/kg)	Recovery (%)
1	93.58	3.32	111.9
2	46.44	1.56	109.4
3	16.89	1.52	99.13
4	7.386	0.923	87.29
5	3.304	0.167	77.08
6	1.248	0.180	73.17

Table 44. RM 8446 Part B fluoride mass fraction results (with blank correction).

Calibration Level	Sample F^- Mass Fraction (mg/kg)	Standard Deviation (mg/kg)	Recovery (%)
1	103.3	2.5	97.49
2	46.71	2.32	88.98
3	17.50	3.56	84.55
4	7.426	0.191	70.72
5	2.948	0.163	57.80
6	0.960	0.122	46.60

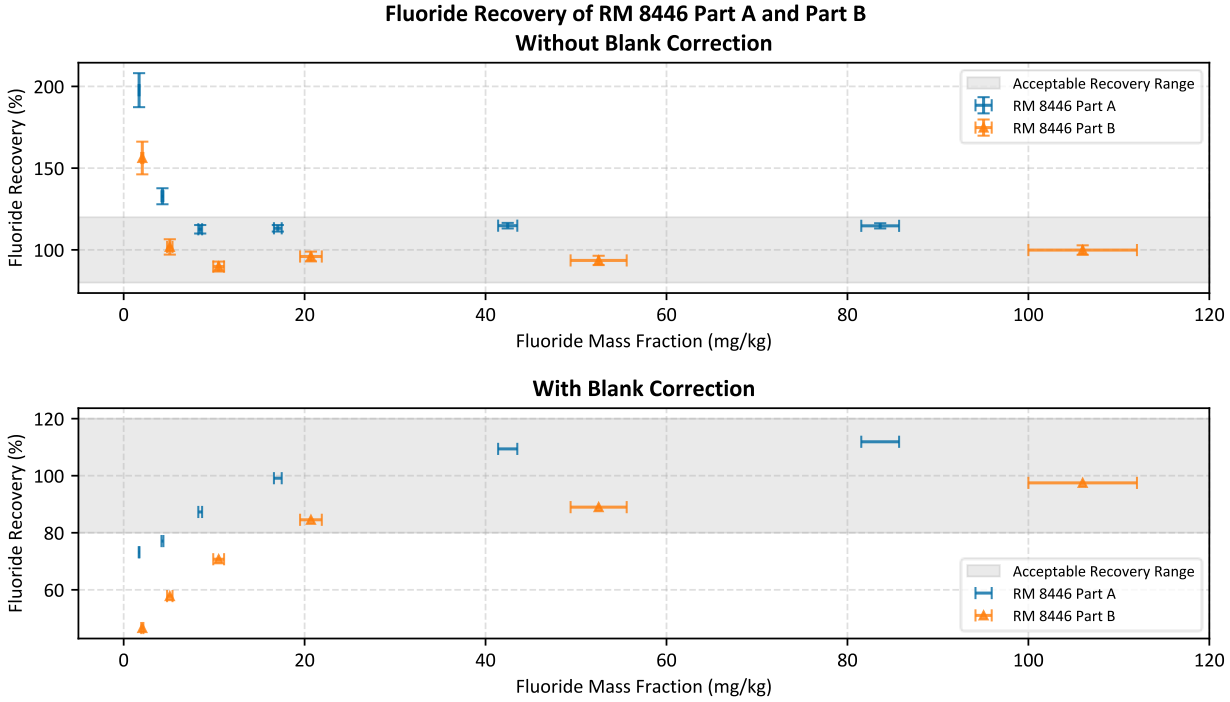

Figure 11. Fluoride recovery rates of RM 8446 with and without blank correction.

All 3rd-party PFAS standards except 8:2 FTOH were within the acceptable fluoride recovery range (**Table 45** and **Figure 12**).

Table 45. Fluoride mass fractions and recovery percentages of 3rd-party PFAS standards (no blank correction).

Compound	Average Sample Combustion Mass (mg)	Expected F^- Mass Fraction (mg/kg)	Measured F^- Mass Fraction (mg/kg)	Recovery (%)
4:2 FTOH	80.28 ± 0.54	40.93 ± 1.62	39.65 ± 0.85	96.86 ± 4.36
5:2 sFTOH	80.33 ± 0.94	42.05 ± 1.66	40.33 ± 1.09	95.91 ± 4.59
8:2 FTOH	81.55 ± 0.40	43.99 ± 1.74	53.44 ± 1.08	121.49 ± 5.40
10:2 FTOH	80.83 ± 0.40	44.70 ± 1.77	50.09 ± 2.55	112.05 ± 7.23
8:2 FTAcr	69.74 ± 0.38	45.04 ± 1.56	40.41 ± 0.88	89.72 ± 3.67

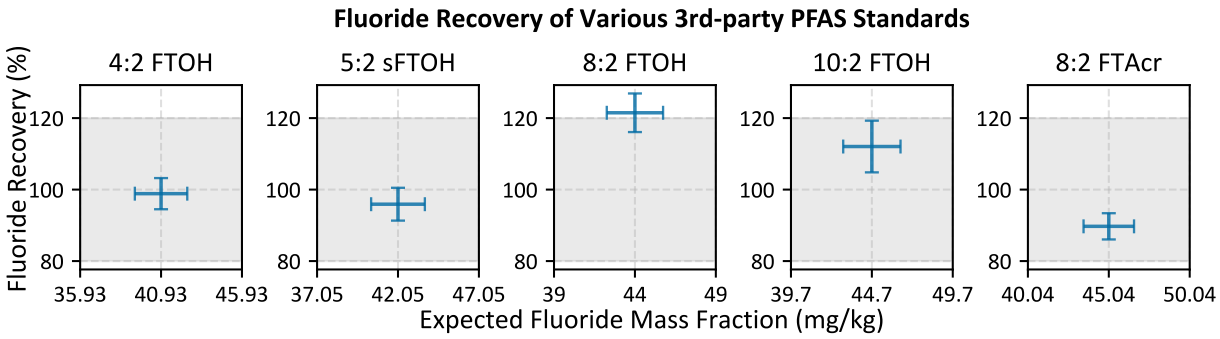

Figure 12. Fluoride recovery of 3rd-party PFAS standards (no blank correction).

For solutions containing SRM 2143 and SRM 2144, recovery values were below the expected values, except at calibration levels with lower expected elemental concentrations (**Tables 46 and 47**). When blank-corrected with water blanks (**Table 48**), fluoride mass fractions (**Table 49**) were lower overall, with all fluoride mass fractions below 100 % and most chloride mass fractions (**Table 50**) below 100 % (except for calibration levels 5, 6, and 7 as seen in **Figure 13**). This may be attributed to the overall lower sensitivity for chlorine using this method.

Table 46. Fluoride mass fraction in solutions containing SRM 2143 and SRM 2144 (no blank correction).

Calibration Level	Sample F^- Mass Fraction (mg/kg)	Mass Fraction Standard Deviation (mg/kg)	Recovery (%)
1	111.6 ± 2.4	3.0	93.42 ± 1.06
2	53.66 ± 1.20	0.65	91.09 ± 0.46
3	27.96 ± 0.62	0.35	93.59 ± 0.24
4	21.41 ± 0.48	0.44	90.61 ± 0.18
5	10.79 ± 0.26	0.41	92.68 ± 0.10
6	5.723 ± 0.164	0.11	99.53 ± 0.04
7	2.771 ± 0.122	0.07	114.7 ± 3.0

Table 47. Chloride mass fraction in solutions containing SRM 2143 and SRM 2144 (no blank correction).

Calibration Level	Sample Cl^- Mass Fraction (mg/kg)	Mass Fraction Standard Deviation (mg/kg)	Recovery (%)
1	114.9 ± 2.6	2.6	94.72 ± 2.20
2	55.61 ± 1.26	0.63	92.96 ± 2.18
3	28.21 ± 0.66	0.33	92.99 ± 2.26
4	21.87 ± 0.54	0.66	91.14 ± 2.28
5	12.80 ± 0.38	0.93	108.3 ± 3.2
6	7.784 ± 0.292	1.53	133.3 ± 5.0
7	3.421 ± 0.252	0.045	139.4 ± 10.4

Table 48. Averaged apparent fluoride and chloride concentration of adsorption solution of water blanks (N=3).

Anion	Apparent Concentration (mg/µL)	Standard Deviation (mg/µL)	IC Injection Volume (µL)
F^-	1.553×10^{-9}	6.803×10^{-12}	200
Cl^-	3.543×10^{-9}	2.224×10^{-11}	

Table 49. Fluoride mass fraction in solutions containing SRM 2143 and SRM 2144 (with blank correction).

Calibration Level	Sample F^- Mass Fraction (mg/kg)	Standard Deviation (mg/kg)	Recovery (%)
1	111.5	3.0	93.34
2	53.57	0.65	90.93
3	27.87	0.35	93.27
4	21.32	0.44	90.21
5	10.69	0.41	91.84
6	5.630	0.109	97.91
7	2.679	0.073	96.66

Table 50. Chloride mass fraction in solutions containing SRM 2143 and SRM 2144 (with blank correction).

Calibration Level	Sample Cl^- Mass Fraction (mg/kg)	Standard Deviation (mg/kg)	Recovery (%)
1	114.7	2.6	94.54
2	55.40	0.63	92.60
3	28.00	0.33	92.29
4	21.66	0.67	90.25
5	12.57	0.95	106.4
6	7.572	1.547	129.6
7	3.210	0.044	130.8

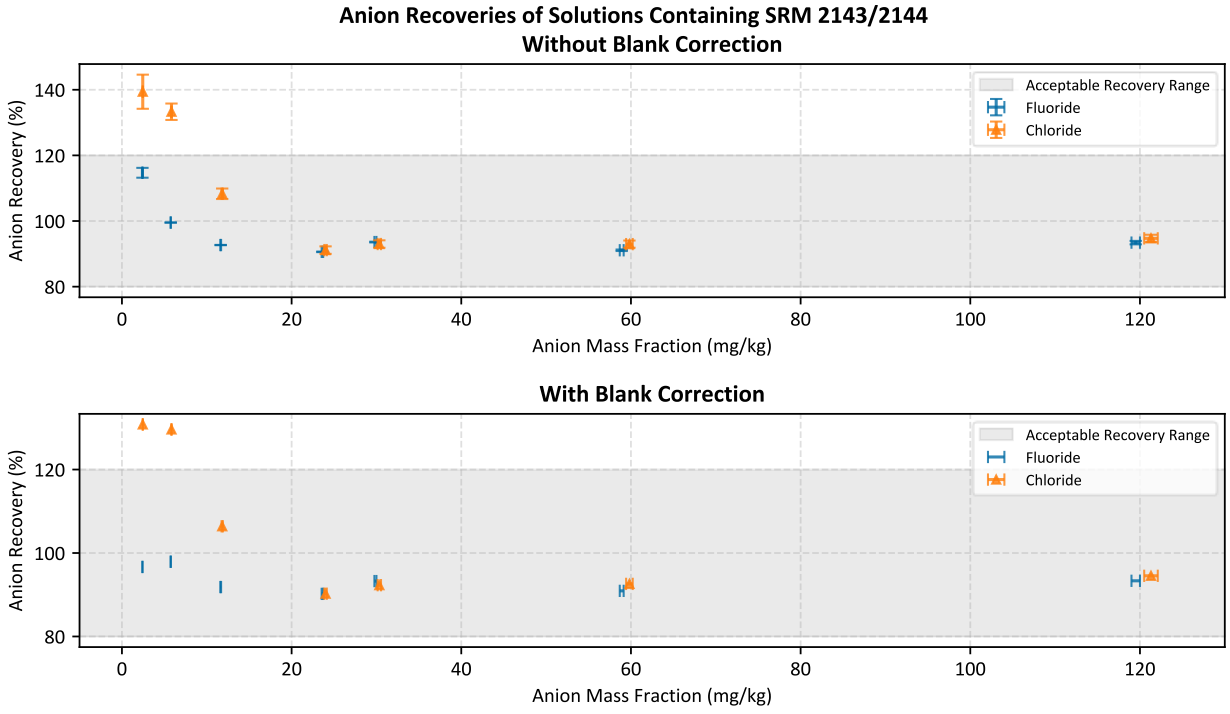

Figure 13. Anion recovery rates of SRM 2143/2144 solutions.

4.4. Effects of Cations on Fluorine Measurements

Tables 51 and 52 list the fluoride recoveries of solutions containing cation SRMs 3129a or 3109a in addition to fluoride SRM 3183. As seen in **Figure 14**, all cation to fluoride ratios showed recoveries within the acceptable range of 80 % to 120 %. A small decrease in recoveries is noted in solutions with cation to fluoride ratios higher than unity, which could indicate the formation of insoluble salts such as calcium fluoride.

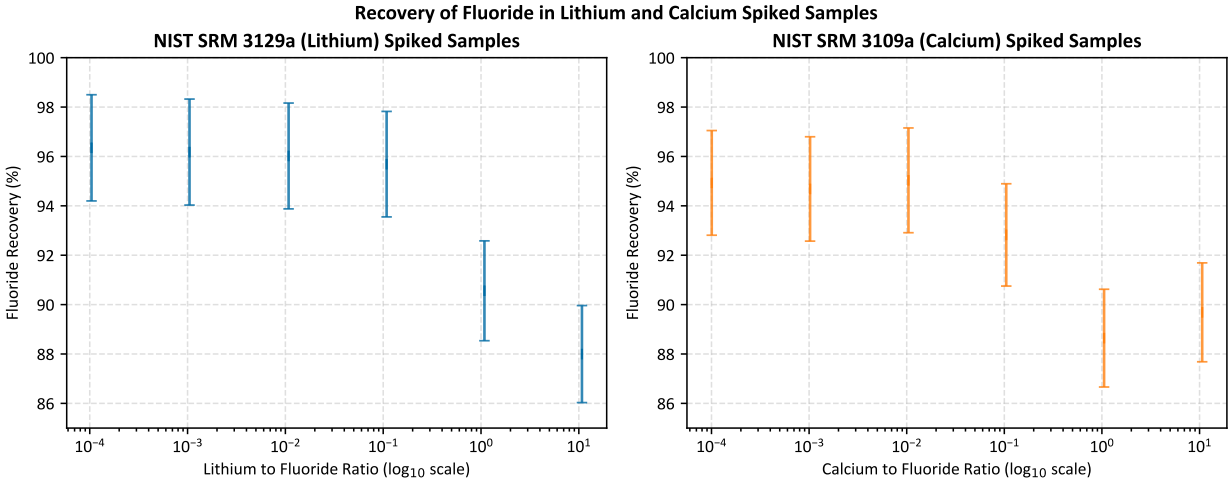

Figure 14. Fluoride recoveries of lithium/calcium spiked samples (k=2, no blank correction).

Table 51. Expected and measured mass fractions of lithium cation and fluoride anions (k=2).

Solution	Expected F^- Mass Fraction (mg/kg)	Measured F^- Mass Fraction (mg/kg)	Fluoride Recovery (%)
LiF 1	98.20 ± 0.31	86.41 ± 1.91	88.00 ± 1.97
LiF 2	98.92 ± 0.31	89.58 ± 1.98	90.56 ± 2.02
LiF 3	98.17 ± 0.31	93.94 ± 2.08	95.69 ± 2.14
LiF 4	98.68 ± 0.31	94.75 ± 2.09	96.02 ± 2.14
LiF 5	99.27 ± 0.31	95.48 ± 2.11	96.18 ± 2.15
LiF 6	98.76 ± 0.31	95.15 ± 2.1	96.35 ± 2.15
LiF 7	99.89 ± 0.31	94.68 ± 2.09	94.79 ± 2.12

Table 52. Expected and measured mass fractions of calcium cation and fluoride anions in each solution (k=2).

Solution	Expected F^- Mass Fraction (mg/kg)	Measured F^- Mass Fraction (mg/kg)	Fluoride Recovery (%)
CaF 1	98.70 ± 0.31	88.52 ± 1.96	89.69 ± 2.00
CaF 2	99.64 ± 0.31	88.32 ± 1.95	88.64 ± 1.98
CaF 3	99.86 ± 0.31	92.69 ± 2.05	92.82 ± 2.07
CaF 4	99.12 ± 0.31	94.2 ± 2.08	95.03 ± 2.12
CaF 5	99.38 ± 0.31	94.1 ± 2.08	94.68 ± 2.11
CaF 6	98.20 ± 0.31	93.22 ± 2.06	94.93 ± 2.12
CaF 7	98.81 ± 0.31	95.17 ± 2.10	96.31 ± 2.15

4.5. Concurrent Sulfur Determinations

The hydrogen peroxide concentration of the absorber solution was lowered from 500 mg/kg to 100 mg/kg. To verify that this concentration allows for the accurate measurement of sulfur in complex mixtures while maintaining the ability to measure halides, SRM 1635a and SRM 1646a were combusted (**Table 53**). Values in parenthesis ( ) denote values below the limit of quantitation and values in parenthesis followed by asterisks ( )* denote numbers above the maximum calibration level.

For SRM 1635a, we observed an excellent agreement with CANSPEX interlaboratory study value for fluorine (63 mg/kg) and a poor agreement with chlorine values (51 mg/kg). Bromine values were higher than the reported mass fraction value of interest of 1 mg/kg, which could be attributed to the value being below the limit of quantitation. Sulfur values could not be accurately determined as they were over the highest calibration level, but it nevertheless was within the same order of magnitude as the certified value.

To quantify SRM 1646a, low combustion masses were required. Nonetheless, the sulfur mass fraction was near the certified value of 0.352×10^4 mg/kg. The validity of the SRM 1646a halide mass fractions could not be determined at this time as no halogen mass fractions were reported for SRM 1646a.

Table 53. Mass fractions of solid NIST SRMs using 100 mg/kg hydrogen peroxide in water as the absorber solution.

SRM	Average Combustion Mass (mg, N=3)	F^- (mg/kg)	Cl^- (mg/kg)	Br^- (mg/kg)	SO_4^- (mg/kg)	Sulfur (mg/kg)
1635a	101.49 ± 1.44	62.25 ± 1.19	11.13 ± 0.26	(2.68)	(5.92×10^4) *	(1.96×10^3) *
1646a	1.62 ± 0.15	305.2 ± 8.8	7575 ± 148	(144.7)	$1.17 \times 10^4 \pm 2 \times 10^2$	$3.89 \times 10^3 \pm 5 \times 10^2$

5. Discussion

This report presents a method to measure halogen and sulfur content in complex matrices and a rigorous method to estimate measurement uncertainty. While traditional IC has a small linear range, this method presents a workaround with the ability to change both combustion mass and IC injection volume to increase the effective measurement range. However, additional work on the characterization of the partial loop injection approach is warranted. The uncertainty estimation method presented in this report is likely to overestimate the uncertainty values, as it implicitly includes other environmental factors such as, but not limited to, temperature fluctuations, eluent/absorption solution strength, and background contamination of UPW. Inclusion of these environmental variables in future studies would allow for a more rigorous quantification of the uncertainty for the nominal halogen values reported through this method.

It appears that the uncertainty originating from the calibration curve fit generation dominates overall sample mass fraction uncertainty, but more information is required to validate this assumption. In addition, more information on the drift and stability of the instrument is needed. While the technical specifications suggest that drift is not an issue, it may be good practice to verify and correct future measurements using this method.

For calibration curves created using organic halogenated compounds, careful selection of the certified reference materials (CRM) is required. Specifically, calibration curves created via the combustion of organofluorines, and even inorganic fluoride appear much steeper than the direct injection method used in this report. This could be due to a myriad of reasons, such as impurities in the CRMs, fluoride contamination from glassware used to contain said CRMs, and interferences from organic compounds created during combustion. At this time, the mechanism is unclear. For organochlorines and combustion of chloride, a lower slope was observed, likely related to chloride loss during the combustion process.

Many of the results found in this report, particularly PFAS measurements, are limited by the chemical purity of CRMs. While the chemical purity of all reference materials used in this study were 98 % or higher, the storage method of these CRMs (especially when shipped in amber glass vials) may allow for the diffusion of fluoride from the glass into the bulk solution. This may explain how PFAS combustion efficiencies are above 100 % in many cases. This is contrasted by less than 100 % recovery rates of SRM 3183 (fluoride anion) which comes in a high-density polyethylene bottle (see **Figure 14** and **Tables 51 and 52**). At this time, it is difficult to compare our PFAS combustion efficiencies to preexisting, published values as only 8:2 FTOH combustion efficiencies were found [58]. It is our understanding that this is the first publication of the combustion efficiency/recovery rate of NIST RM 8446 and SRM 2143.

Although all fluoride anion recoveries were within our acceptable range of 80 % to 120 %, the lower fluoride recovery rates for cation (lithium and calcium) spiked solutions are a concern. This contrasts with literature, where PFAS was used as the source of fluorine instead of fluoride anion [58]. However, this may be irrelevant for many experimenters, as this effect is most prominent in extremely high concentrations. It is likely that the ordinary experimenter will be more concerned with the probable damage to quartz consumables (quartz tube, boats, hooks, filters, etc.) than the decrease in the recovery.

Excellent sulfur recovery was observed with concurrence with excellent fluoride recovery. In future studies, the lowered hydrogen peroxide concentration will be used as the absorber solution. The higher concentration did not appear to affect any halide measurements, as all analytical runs for this report passed our set calibration checks.

Further examinations of the fate of both organic and inorganic fluorinated compounds throughout our PFAS extractions are underway. Our scope currently includes determining total fluorine (TF), extracted organofluorines (EOF), adsorbed organofluorines (AOF), and unextracted organofluorines (UOF) in firefighter gear textiles and soot collected from the combustion of household textiles. This includes the study of solvent selection on the EOF content of the final extracts.

In addition, work is underway to determine halogen content of previously reported and newly purchased firefighter gear textiles. It is important to note that samples containing fluoropolymers may not be easily measured without compromising sample homogeneity, due to their high concentrations of halogens. For example, textiles made primarily of fluoropolymers may contain high concentrations of fluorine that can easily exceed the calibration range of the method, even with sub-milligram combustion masses. In such cases, more replicates may be necessary or made clear that the measurements may not be representative of the overall sample halogen content. Alternative sample preparation methods such as cryogenic grinding to ensure heterogeneity may be useful but were not explored in this report.

5.1. Recommended Best Practices

Though more work on the characterization of this method is needed, the following recommendations for CIC-based total fluorine measurements of PFAS are offered based on our current understanding:

1. **Calibration**: Fit both linear and quadratic response model for each analyte. Do not rely on R^2 values alone, because they can mask systematic biases in certain on-column mass regions.
2. **Injection volume**: The relative uncertainty of the injection volume is larger for smaller injection volumes. Consequently, use the highest injection volume possible for the sample (sample dilution may be necessary). Determine the uncertainty for each injection-volume set point by pyrohydrolyzing replicates of a calibration standard (e.g., check standard 4) and calculating the standard deviation of those replicates.
3. **Blank correction**: Perform blank subtraction only for samples that were injected with the same volume set point as the corresponding blank.
4. **Glassware**: See **Appendix E**. A dedicated cleaning procedure for glassware may be required to lower the background fluoride to an acceptable level.

6. References

[1] Brinchmann BC, Bugge MD, Nordby K-C, Alfonso JH (2022) Firefighting and melanoma, epidemiological and toxicological associations: a case report. *Occupational Medicine (Oxford, England)* 72(2):142–144. https://doi.org/10.1093/occmed/kqab183

[2] Pálešová N, Maitre L, Stratakis N, Řiháčková K, Pindur A, Kohoutek J, Šenk P, Bartošková Polcrová A, Gregor P, Vrijheid M, Čupr P (2023) Firefighters and the liver: Exposure to PFAS and PAHs in relation to liver function and serum lipids (CELSPAC-FIREexpo study). *International Journal of Hygiene and Environmental Health* 252:114215. https://doi.org/10.1016/j.ijheh.2023.114215

[3] Alexander BM, Baxter CS (2016) Flame-retardant contamination of firefighter personal protective clothing – A potential health risk for firefighters. *Journal of Occupational and Environmental Hygiene* 13(9):D148–D155. https://doi.org/10.1080/15459624.2016.1183016

[4] Mazumder N-U-S, Hossain MT, Jahura FT, Girase A, Hall AS, Lu J, Ormond RB (2023) Firefighters' exposure to per-and polyfluoroalkyl substances (PFAS) as an occupational hazard: A review. *Frontiers in Materials* 10. https://doi.org/10.3389/fmats.2023.1143411

[5] Maizel A, Thompson A, Tighe M, Escobar Veras S, Rodowa A, Falkenstein-Smith R, Benner Jr BA, Hoffman K, Donnelly MK, Hernandez O, Wetzler N, Ngu T, Reiner J, Place B, Kucklick J, Rimmer K, Davis RD (2023) Per- and polyfluoroalkyl substances in new firefighter turnout gear textiles. (National Institute of Standards and Technology (U.S.), Gaithersburg, MD), NIST TN 2248, p NIST TN 2248. https://doi.org/10.6028/NIST.TN.2248

[6] Maizel A, Thompson A, Place B, Rodowa A, Reiner J, Tombaugh A, Solomon H, Stinger B, Donnelly M, Davis R (2025) Suspect Screening of Per- and Polyfluoroalkyl Substances in New Firefighter Turnout Gear Textiles. (National Institute of Standards and Technology, Gaithersburg, MD), NIST TN 2334, p NIST TN 2334. https://doi.org/10.6028/NIST.TN.2334

[7] Muensterman DJ, Titaley IA, Peaslee GF, Minc LD, Cahuas L, Rodowa AE, Horiuchi Y, Yamane S, Fouquet TNJ, Kissel JC, Carignan CC, Field JA (2022) Disposition of Fluorine on New Firefighter Turnout Gear. *Environmental Science & Technology* 56(2):974–983. https://doi.org/10.1021/acs.est.1c06322

[8] Aliaño-González MJ, Montalvo G, García-Ruiz C, Ferreiro-González M, Palma M (2022) Assessment of Volatile Compound Transference through Firefighter Turnout Gear. *International Journal of Environmental Research and Public Health* 19(6):3663. https://doi.org/10.3390/ijerph19063663

[9] Thompson AL, Maizel A, Tighe M, Escobar Veras S, Rodowa A, Benner B, Tombaugh A, Reiner J, Donnelly M, Falkenstein-Smith R, Kucklick J, Rimmer C, Davis R (2024) Per- and polyfluoroalkyl substances in textiles present in firefighter gloves, hoods, and wildland gear. (National Institute of Standards and Technology (U.S.), Gaithersburg, MD), NIST TN 2313, p NIST TN 2313. https://doi.org/10.6028/NIST.TN.2313

[10] Levasseur JL, Hoffman K, Herkert NJ, Cooper E, Hay D, Stapleton HM (2022) Characterizing firefighter's exposure to over 130 SVOCs using silicone wristbands: A pilot study comparing on-duty and off-duty exposures. *Science of The Total Environment* 834:155237. https://doi.org/10.1016/j.scitotenv.2022.155237

[11] Laitinen JA, Koponen J, Koikkalainen J, Kiviranta H (2014) Firefighters' exposure to perfluoroalkyl acids and 2-butoxyethanol present in firefighting foams. *Toxicology Letters* 231(2):227–232. https://doi.org/10.1016/j.toxlet.2014.09.007
[12] Antoniou EE, Dekant W (2024) Childhood PFAS exposure and immunotoxicity: a systematic review and meta-analysis of human studies. *Systematic Reviews* 13(1):176. https://doi.org/10.1186/s13643-024-02596-z
[13] Cao Y, Ng C (2021) Absorption, distribution, and toxicity of per- and polyfluoroalkyl substances (PFAS) in the brain: a review. *Environmental Science Processes & Impacts* 23(11):1623–1640. https://doi.org/10.1039/d1em00228g
[14] Ermler S, Kortenkamp A (2022) Systematic review of associations of polychlorinated biphenyl (PCB) exposure with declining semen quality in support of the derivation of reference doses for mixture risk assessments. *Environmental Health: A Global Access Science Source* 21(1):94. https://doi.org/10.1186/s12940-022-00904-5
[15] Rengelshausen J, Randerath I, Schettgen T, Esser A, Kaifie A, Lang J, Kraus T, Ziegler P (2023) Ten years after: findings from the medical surveillance program on Health Effects in High-Level Exposure to PCB (HELPcB). *Archives of Toxicology* 97(10):2609–2623. https://doi.org/10.1007/s00204-023-03578-1
[16] Estimation of the health risks associated with polychlorinated biphenyl (PCB) concentrations found onboard older U.S. Navy vessels - PubMed Available at https://pubmed.ncbi.nlm.nih.gov/12959885/
[17] Gomes J, Begum M, Kumarathasan P (2024) Polybrominated diphenyl ether (PBDE) exposure and adverse maternal and infant health outcomes: Systematic review. *Chemosphere* 347:140367. https://doi.org/10.1016/j.chemosphere.2023.140367
[18] Liu B, Lehmler H-J, Ye Z, Yuan X, Yan Y, Ruan Y, Wang Y, Yang Y, Chen S, Bao W (2024) Exposure to Polybrominated Diphenyl Ethers and Risk of All-Cause and Cause-Specific Mortality. *JAMA network open* 7(4):e243127. https://doi.org/10.1001/jamanetworkopen.2024.3127
[19] Jacob P, Barzen-Hanson KA, Helbling DE (2021) Target and Nontarget Analysis of Per- and Polyfluoralkyl Substances in Wastewater from Electronics Fabrication Facilities. *Environmental Science & Technology* 55(4):2346–2356. https://doi.org/10.1021/acs.est.0c06690
[20] Joseph NT, Schwichtenberg T, Cao D, Jones GD, Rodowa AE, Barlaz MA, Charbonnet JA, Higgins CP, Field JA, Helbling DE (2023) Target and Suspect Screening Integrated with Machine Learning to Discover Per- and Polyfluoroalkyl Substance Source Fingerprints. *Environmental Science & Technology* 57(38):14351–14362. https://doi.org/10.1021/acs.est.3c03770
[21] Chibwe L, De Silva AO, Spencer C, Teixera CF, Williamson M, Wang X, Muir DCG (2023) Target and Nontarget Screening of Organic Chemicals and Metals in Recycled Plastic Materials. *Environmental Science & Technology* 57(8):3380–3390. https://doi.org/10.1021/acs.est.2c07254
[22] Croley TR, White KD, Callahan JH, Musser SM (2012) The Chromatographic Role in High Resolution Mass Spectrometry for Non-Targeted Analysis. *Journal of the American Society for Mass Spectrometry* 23(9):1569–1578. https://doi.org/10.1007/s13361-012-0392-0

[23] Renai L, Del Bubba M, Gargano AFG, Samanipour S (2024) Consolidating two-dimensional liquid chromatography–high-resolution tandem mass spectrometry (LC×LC-HRMS/MS) technique for the non-targeted analysis of poly- and perfluorinated substances: A trial on aqueous film-forming foams. *Science of The Total Environment* 952:175908. https://doi.org/10.1016/j.scitotenv.2024.175908

[24] Humbert K, Debret M, Morin C, Cosme J, Portet-Koltalo F (2022) Direct thermal desorption-gas chromatography-tandem mass spectrometry versus microwave assisted extraction and GC-MS for the simultaneous analysis of polyaromatic hydrocarbons (PAHs, PCBs) from sediments. *Talanta* 250:123735. https://doi.org/10.1016/j.talanta.2022.123735

[25] Dmitrovic J, Chan SC, Chan SHY (2002) Analysis of pesticides and PCB congeners in serum by GC/MS with SPE sample cleanup. *Toxicology Letters* 134(1):253–258. https://doi.org/10.1016/S0378-4274(02)00173-X

[26] Zhao L, Xu C, Parry E, Giardina M (2025) Determination of per- and polyfluoroalkyl substances in tissue using QuEChERS extraction followed by novel enhanced matrix removal mixed-mode passthrough cleanup with LC-MS/MS detection. *Journal of Chromatography A* 1758:466150. https://doi.org/10.1016/j.chroma.2025.466150

[27] Miserli K, Athanasiou V, Boti V, Hela D, Konstantinou I (2023) Determination of PFAS in wastewaters and natural waters by solid phase extraction and UHPLC LTQ/Orbitrap MS for assessing occurrence and removals. *Case Studies in Chemical and Environmental Engineering* 8:100505. https://doi.org/10.1016/j.cscee.2023.100505

[28] Fung YS, Dao KL (1996) Elemental analysis of chemical wastes by oxygen bomb combustion-ion chromatography. *Analytica Chimica Acta* 334(1):51–56. https://doi.org/10.1016/S0003-2670(96)00320-0

[29] Fung YS, Wu Z, Dao KL (1996) Determination of Total Organic Carbon in Water by Thermal Combustion-Ion Chromatography. *Analytical Chemistry* 68(13):2186–2190. https://doi.org/10.1021/ac951146x

[30] Miyake Y, Kato M, Urano K (2007) A method for measuring semi- and non-volatile organic halogens by combustion ion chromatography. *Journal of Chromatography A* 1139(1):63–69. https://doi.org/10.1016/j.chroma.2006.10.078

[31] Gokhale D, Cerrón-Calle GA, Kim-Fu ML, Flores K, Román Santiago A, Tsai S-W, Aga DS, Aich N, Diallo MS, Doudrick K, Hanigan D, Hernández Sánchez R, Howarter J, Jiang J "Jimmy," Jones GD, Lee LS, Liu H, Manz KE, McKenzie ER, Padhye LP, Sankaran RM, Shepard SM, Strathmann TJ, Venkatesan AK, Wong MS, Leet R, Speed D, Field JA, Westerhoff P, Su X (2026) Challenges and Opportunities in PFAS Waste Management for Semiconductor Manufacturing. *Environmental Science & Technology* 60(3):2259–2276. https://doi.org/10.1021/acs.est.5c10109

[32] Allgood CC (2003) Fluorinated gases for semiconductor manufacture: process advances in chemical vapor deposition chamber cleaning. *Journal of Fluorine Chemistry* 122(1):105–112. https://doi.org/10.1016/S0022-1139(03)00101-5

[33] Chen Y-J, Yang J-S, Lin AY-C (2024) Comprehensive nontargeted analysis of fluorosurfactant byproducts and reaction products in wastewater from semiconductor manufacturing. *Sustainable Environment Research* 34(1):14. https://doi.org/10.1186/s42834-024-00221-1

[34] Kim J, Hwang Y, Yoo M, Chen S, Lee I-M (2017) Hydrogen fluoride (HF) substance flow analysis for safe and sustainable chemical industry. *Environmental Science and Pollution Research* 24(32):25137–25145. https://doi.org/10.1007/s11356-017-0152-6
[35] US EPA Method 1621 Determination of Adsorbable Organic Fluorine (AOF) in Aqueous Matrices by Combustion Ion Chromatography (CIC).
[36] Claassen M, Bingham B, Chow JC, Watson JG, Wang Y, Wang X (2024) Characterization of Lithium-Ion Battery Fire Emissions—Part 1: Chemical Composition of Fine Particles (PM2.5). *Batteries* 10(9):301. https://doi.org/10.3390/batteries10090301
[37] Aro R, Eriksson U, Kärrman A, Reber I, Yeung LWY (2021) Combustion ion chromatography for extractable organofluorine analysis. *iScience* 24(9):102968. https://doi.org/10.1016/j.isci.2021.102968
[38] Wang J, Abusallout I, Song M, Marfil-Vega R, Hanigan D (2021) Quantification of per- and polyfluoroalkyl substances with a modified total organic carbon analyzer and ion chromatography. *AWWA Water Science* 3(4):e1235. https://doi.org/10.1002/aws2.1235
[39] National Institute of Standards and Technology; U.S. Department of Commerce (2022) *SRM 3181; Sulfate Anion (SO42-) Standard Solution* (Gaithersburg, MD).
[40] National Institute of Standards and Technology; U.S. Department of Commerce (2020) *SRM 3182; Chloride Anion (Cl-) Standard Solution* (Gaithersburg, MD).
[41] National Institute of Standards and Technology; U.S. Department of Commerce (2016) *SRM 3183; Fluoride Anion (F–) Standard Solution* (National Institute of Standards and Technology; U.S. Department of Commerce, Gaithersburg, MD).
[42] National Institute of Standards and Technology; U.S. Department of Commerce (2016) *SRM 3184; Bromide Anion (Br-) Standard Solution* (Gaithersburg, MD).
[43] National Institute of Standards and Technology; U.S. Department of Commerce (2021) *SRM 3186; Phosphate Anion (PO43-) Standard Solution* (Gaithersburg, MD).
[44] National Institute of Standards and Technology; U.S. Department of Commerce (2022) *SRM 3129a; Lithium (Li) Standard Solution* (Gaithersburg, MD).
[45] National Institute of Standards and Technology; U.S. Department of Commerce (2021) *SRM 3109a; Calcium (Ca) Standard Solution* (Gaithersburg, MD).
[46] National Institute of Standards and Technology; U.S. Department of Commerce (2023) *RM 8446; Perfluorinated Carboxylic Acids and Perfluorooctane Sulfonamide in Methanol* (Gaithersburg, MD).
[47] National Bureau of Standards (National Institute of Standards and Technology); U.S. Department of Commerce (1982) *SRM 2143; p-Fluorobenzoic Acid* (Washington, DC).
[48] National Bureau of Standards (National Institute of Standards and Technology); U.S. Department of Commerce (1973) *SRM 2144; m-Chlorobenzoic Acid* (Washington, DC).
[49] National Institute of Standards and Technology; U.S. Department of Commerce (2023) *SRM 1635a; Trace Elements of Coal (Subbituminous)* (Gaithersburg, MD).
[50] National Institute of Standards and Technology; U.S. Department of Commerce (2004) *SRM 1646a; Estuarine Sediment* (Gaithersburg, MD).
[51] Newville M, Otten R, Nelson A, Stensitzki T, Ingargiola A, Allan D, Fox A, Carter F, Rawlik M (2025) LMFIT: Non-Linear Least-Squares Minimization and Curve-Fitting for Python. https://doi.org/10.5281/zenodo.16175987

[52] Keunchkarian S, Reta M, Romero L, Castells C (2006) Effect of sample solvent on the chromatographic peak shape of analytes eluted under reversed-phase liquid chromatogaphic conditions. *Journal of Chromatography A* 1119(1–2):20–28. https://doi.org/10.1016/j.chroma.2006.02.006

[53] Toman B, Nelson MA, Bedner M (2017) Rigorous evaluation of chemical measurement uncertainty: Liquid chromatographic analysis methods using detector response factor calibration. *Metrologia* 54(3):S16. https://doi.org/10.1088/1681-7575/aa6404

[54] Yuan Z, Suzuki K, Yamamoto Y, Yajima T, Kawajiri Y (2025) Estimation and Uncertainty Quantification of Solvent Strength Parameters in Gradient Elution of Chromatography Using Sequential Monte Carlo Method. *Processes* 13(1):114. https://doi.org/10.3390/pr13010114

[55] Barwick VJ, Ellison SLR, Lucking CL, Burn MJ (2001) Experimental studies of uncertainties associated with chromatographic techniques. *Journal of Chromatography A* 918(2):267–276. https://doi.org/10.1016/S0021-9673(01)00679-3

[56] Piston-operated volumetric apparatus - Part 3: Burettes (ISO 8655-3:2022) (2022) Available at https://www.iso.org/standard/68798.html

[57] Linstrom P (1997) NIST Chemistry WebBook, NIST Standard Reference Database 69. https://doi.org/10.18434/T4D303

[58] Aro R, Eriksson U, Kärrman A, Reber I, Yeung LWY (2021) Combustion ion chromatography for extractable organofluorine analysis. *iScience* 24(9):102968. https://doi.org/10.1016/j.isci.2021.102968

Appendix A. Reference Data

A.1. Values of Select NIST RM/SRMs

A.1.1. NIST SRM 1635a

Table 54. Certified Mass Fraction Values (Dry-Mass Basis) for SRM 1635a.

Element	Constituent Type	Certified Value (mg/kg)	Expanded Uncertainty (k=2, mg/kg)
Barium (Ba)	Minor	357.8	9.1
Sulfur (S)	Minor	2909	80
Iron (Fe)	Minor	2472	22
Strontium (Sr)	Minor	160	11
Sodium (Na)	Minor	1031	7.8×10^{-3}
Antimony (Sb)	Trace	0.251	0.036
Mercury (Hg)	Trace	0.0836	6.4×10^{-3}
Arsenic (As)	Trace	0.860	0.019
Nickel (Ni)	Trace	5.37	0.30
Chromium (Cr)	Trace	3.56	0.18
Rubidium (Rb)	Trace	1.226	0.043
Cobalt (Co)	Trace	2.004	0.044
Selenium (Se)	Trace	0.662	0.096
Copper (Cu)	Trace	11.42	0.74
Thorium (Th)	Trace	1.299	0.059
Lead (Pb)	Trace	2.85	0.37
Uranium (U)	Trace	0.4792	9.0×10^{-3}
Manganese (Mn)	Trace	6.69	0.14
Vanadium (V)	Trace	13.34	0.59

Table 55. Non-Certified Mass Fraction Values (Dry-Mass Basis) for SRM 1635a.

Element	Constituent Type	Certified Value (mg/kg)	Expanded Uncertainty (mg/kg)	Coverage Factor (k)
Aluminum (Al)	Major	5437	63	2
Magnesium (Mg)	Major	2303	31	2
Calcium (Ca)	Major	1.087×10^4	140	2
Potassium (K)	Major	187.4	7.9	2
Hydrogen (H)	Major	3.92×10^4	2700	2
Titanium (Ti)	Major	0.05240	9.0×10^{-4}	2.05
Boron (B)	Trace	36.0	1.25	2
Hafnium (Hf)	Trace	3.14	0.23	2.11
Cadmium (Cd)	Trace	0.062	0.020	1.95
Molybdenum (Mo)	Trace	6.36	0.97	2.36
Cerium (Ce)	Trace	5.45	0.10	2.09
Samarium (Sm)	Trace	0.483	0.017	2.36
Cesium (Cs)	Trace	0.0998	4.1×10^{-3}	2
Scandium (Sc)	Trace	1.240	0.017	2
Chlorine (Cl)	Trace	15.4	3.0	2
Zinc (Zn)	Trace	7.3	1.5	2
Europium (Eu)	Trace	0.1115	2.1×10^{-3}	2.18

Table 56. Mass Fraction Value of Interest (Dry Mass Basis) for SRM 1635a.

Element	Value (mg/kg)
Bromine (Br)	1

Table 57. Select Values from SRM 1635a CANSPEX Interlaboratory Study Results.

Parameter	Most Likely Value	95 % Coverage Interval of Mean Value	Pooled Within Lab Standard Deviation (s_w)	Pooled Between Lab Standard Deviation (s_B)	Total Number of Labs
Moisture %	20.54	0.15	0.1	0.59	118
Ash % dry basis	6.29	0.045	0.063	0.184	119
Volatile % dry basis	44.75	0.46	0.3	1.59	92
Btu/lb dry basis	11664	19	25	74	110
Carbon % dry basis	68.97	0.34	0.25	0.89	52
Hydrogen % dry basis	4.642	0.135	0.058	0.32	47
Nitrogen % dry basis	0.946	0.051	0.029	0.127	48
Total Sulfur % dry basis	0.294	0.006	0.008	0.022	112
Pyritic Sulfur % dry basis	0.02	0.005	0.002	0.007	16
Sulfate Sulfur % dry basis	0.009	0.005	0.001	0.004	13
Chlorine µg/g dry basis	51	19	8	41	41
Fluorine µg/g dry basis	63	11	5	22	31
Mercury ng/g dry basis	76	9	4	16	28
Selenium µg/g dry basis	0.94	0.79	0.12	0.78	12

A.1.2. NIST SRM 1646a

Table 58. Certified Values for NIST SRM 1646a.

Element	Certified Value (mg/kg)	Expanded Uncertainty (k=2, mg/kg)
Aluminum (Al)	2.297×10^4	0.018×10^4
Arsenic (As)	6.23	0.21
Calcium (Ca)	0.519×10^4	0.020×10^4
Cadmium (Cd)	0.148	0.007
Iron (Fe)	2.008×10^4	0.039×10^4
Chromium (Cr)	40.9	1.9
Magnesium (Mg)	0.388×10^4	0.009×10^4
Copper (Cu)	10.01	0.34
Phosphorus (P)	0.027×10^4	0.001×10^4
Lead (Pd)	11.7	1.2
Potassium (K)	0.864×10^4	0.016×10^4
Manganese (Mg)	234.5	2.8
Silicon (Si)	40.00×10^4	0.16×10^4
Selenium (Se)	0.193	0.028
Sodium (Na)	0.741×10^4	0.017×10^4
Vanadium (V)	44.84	0.76
Sulfur (S)	0.352×10^4	0.004×10^4
Zinc (Zn)	48.9	1.6
Titanium (Ti)	0.456×10^4	0.021×10^4

Table 59. Noncertified values for NIST SRM 1646a.

Element	Mass Fraction (mg/kg)
Antimony	0.3
Neodymium	15
Barium	210
Nickel	23
Beryllium	< 1
Rubidium	38
Cerium	34
Scandium	5
Cobalt	5
Silver	< 0.3
Gallium	5
Strontium	68
Lanthanum	17
Thallium	< 0.5
Lithium	18
Thorium	5.8
Mercury	0.04
Tin	1
Molybdenum	1.8
Uranium	2.0

Appendix B. Equations

B.1. Definition of Variables

A

Peak area.

$\boldsymbol{m}$

On-column analyte mass.

$\boldsymbol{a_n}$

n-th order polynomial fitting parameter.

$\mathbf{r(x, y)}$

Correlation coefficient of terms x and y.

$\boldsymbol{u_x}$

Uncertainty of term x.

B.2. Linear Fit Uncertainty

$$u_{m_{analyte}} = \sqrt{\left(\frac{\partial m}{\partial A} \times u_A\right)^2 + \left(\frac{\partial m}{\partial a_1} \times u_{a_1}\right)^2 + \left(\frac{\partial m}{\partial a_0} \times u_{a_0}\right)^2 + 2\frac{\partial m}{\partial a_1}\frac{\partial m}{\partial a_0} u_{a_1} u_{a_0} r(a_1, a_0)}$$

$$= \sqrt{\begin{aligned}&\left(\frac{1}{a_1} \times u_A\right)^2 + \left(-\frac{A - a_0}{a_1^2} \times u_{a_1}\right)^2 + \left(-\frac{1}{a_1} \times u_{a_0}\right)^2 \\ &\quad +2\left(-\frac{A - a_0}{a_1^2}\right)\left(-\frac{1}{a_1}\right) u_{a_1} u_{a_0} r(a_1, a_0)\end{aligned}}$$

B.3. 2nd Order Polynomial Fit Uncertainty

$$u^2_{m_{analyte}} = \left(\frac{\partial m}{\partial A} \times u_A\right)^2 + \left(\frac{\partial m}{\partial a_2} \times u_{a_2}\right)^2 + \left(\frac{\partial m}{\partial a_1} \times u_{a_1}\right)^2 + \left(\frac{\partial m}{\partial a_0} \times u_{a_0}\right)^2$$
$$+2\frac{\partial m}{\partial a_2}\frac{\partial m}{\partial a_1}u_{a_2}u_{a_1}r(a_2,a_1) + 2\frac{\partial m}{\partial a_2}\frac{\partial m}{\partial a_0}u_{a_2}u_{a_0}r(a_2,a_0) + 2\frac{\partial m}{\partial a_1}\frac{\partial m}{\partial a_0}u_{a_1}u_{a_0}r(a_1,a_0)$$

$$= \left(\frac{1}{\sqrt{a_1^2 - 4a_2(a_0 - A)}} \times u_A\right)^2 + \left(-\frac{1}{\sqrt{a_1^2 - 4a_2(a_0 - A)}} * u_{a_2}\right)^2$$
$$+ \left(\frac{-1 + \frac{a_1}{\sqrt{a_1^2 - 4a_2(a_0 - A)}}}{2a_2} \times u_{a_1}\right)^2$$
$$+ \left(\left(\frac{-a_0 + A}{a_2\sqrt{a_1^2 - 4a_2(a_0 - A)}} - \frac{-a_1 + \sqrt{a_1^2 - 4a_2(a_0 - A)}}{2a_2^2}\right) \times u_{a_0}\right)^2$$
$$+ 2\left(-\frac{1}{\sqrt{a_1^2 - 4a_2(a_0 - A)}}\right)\left(\frac{-1 + \frac{a_1}{\sqrt{a_1^2 - 4a_2(a_0 - A)}}}{2a_2}\right)u_{a_2}u_{a_1}r(a_2,a_1)$$
$$+ 2\left(-\frac{1}{\sqrt{a_1^2 - 4a_2(a_0 - A)}}\right)\left(\frac{-a_0 + A}{a_2\sqrt{a_1^2 - 4a_2(a_0 - A)}}\right.$$
$$\left. - \frac{-a_1 + \sqrt{a_1^2 - 4a_2(a_0 - A)}}{2a_2^2}\right)u_{a_2}u_{a_0}r(a_2,a_0)$$
$$+ 2\left(\frac{-1 + \frac{a_1}{\sqrt{a_1^2 - 4a_2(a_0 - A)}}}{2a_2}\right)\left(\frac{-a_0 + A}{a_2\sqrt{a_1^2 - 4a_2(a_0 - A)}}\right.$$
$$\left. - \frac{-a_1 + \sqrt{a_1^2 - 4a_2(a_0 - A)}}{2a_2^2}\right)u_{a_1}u_{a_0}r(a_1,a_0)$$

Appendix C. Analysis Code

C.1. Calibration Curve Creation and Uncertainty Calculations

```
import numpy as np

import matplotlib.pyplot as plt

import lmfit

import pandas as pd


test_cal_concs = [2.019] # Put the calibration solution concentrations here

test_cal_times = ['2025-05-14 18:16:02 UTC-4'] # if there are multiple calibration solution concentrations, put which sample times correspond to when those calibration solutions were changed here


# open .csv file and read data

test_path = r"C:\Users\hds2\PREP-PFAS\CIC\CIC Liquid Injections\CIC 20250624 - IC\CIC 20250624.csv" # Right click on the exported .csv file and click "Copy as path"

test_pd_data = pd.read_csv(test_path, sep=',') # Read in the .csv file

# Drop empty row

test_pd_data.dropna(how='all', inplace=True) # Drop empty rows

test_pd_data.replace(np.nan, 0, inplace=True) # Replace NaN with 0


# Grab file name

file_name = test_path.split('\\')[-1].split('.')[0]

folder_path = '\\'.join(test_path.split('\\')[:-1]) + '\\'


# only keep columns of interest

keep_cols = ['Determination start', 'Sample', 'Sample type', 'Volume (uL)', 'Combustion amount (mg)', 'RS.CV total volume', 'RS.CV combustion time',

        'Fluoride Retention Time (min)', 'Fluoride Peak Area (uS/cm*min)', 'Chloride Retention Time (min)', 'Chloride Peak Area (uS/cm*min)',

        'Bromide Retention Time (min)', 'Bromide Peak Area (uS/cm*min)','Anions.Phosphate.Retention time', 'Anions.Phosphate.Area',

        'Sulfate Retention Time (min)', 'Sulfate Peak Area (uS/cm*min)']

test_pd_data = test_pd_data[keep_cols]


# Rename Anions.Phosphate.Area to Phosphate Peak Area (uS/cm*min)

test_pd_data.rename(columns={'Anions.Phosphate.Area': 'Phosphate Peak Area (uS/cm*min)'}, inplace=True)

# Rename Anions.Phosphate.Retention time to Phosphate Retention Time (min)
```

```
test_pd_data.rename(columns={'Anions.Phosphate.Retention time': 'Phosphate Retention Time (min)'},
inplace=True)


def linear_fit(m,a,b):
    # Function: A = a*m + b
    return a*m + b
def quad_fit(m,a,b,c):
    # Function: A = a*m^2 + b*m + c
    return a*m**2 + b*m + c


def linear_results(A,a,b):
    # Function: A = a*m + b
    return (A-b)/a
def quad_results(A,a,b,c):
    # Function: A = a*m^2 + b*m + c
    return (-b + np.sqrt(b**2 - 4*a*(c - A)))/(2*a)


def lin_fit_unc(A,a,b,uA,ua,ub,uab):
    # A: Peak area
    # a: first order coefficient
    # b: constant coefficient
    # uA: Peak area uncertainty
    # ua: first order coefficient uncertainty
    # ub: constant coefficient uncertainty
    # uab: covariance between first order coefficient and constant coefficient


    dmdA = 1/a
    dmda = (b-A)*a**(-2)
    dmdb = -1/a


    return np.sqrt((dmdA*uA)**2 + (dmda*ua)**2 + (dmdb*ub)**2 + 2*dmda*dmdb*uab)


def quad_fit_unc(A,a,b,c,uA,ua,ub,uc,uab,ubc,uac):


    # A: Peak area
    # a: second order coefficient
```

```
    # b: first order coefficient
    # c: constant coefficient
    # uA: Peak area uncertainty
    # ua: second order coefficient uncertainty
    # ub: first order coefficient uncertainty
    # uc: constant coefficient uncertainty
    # uab: covariance between second order coefficient and first order coefficient
    # uac: covariance between second order coefficient and constant coefficient
    # ubc: covariance between first order coefficient and constant coefficient

    dmdA = (b**2-4*a*c+4*a*A)**(-0.5)
    dmda = -b**2/(2*a**2*(4*a*A-4*a*c+b**2)**0.5) + b/(2*a**2) + (c-A)/(a*(4*a*A-4*a*c+b**2)**0.5)
    dmdb = b/(2*a*(b**2-4*a*c+4*a*A)**0.5) - 1/(2*a)
    dmdc = -1/(b**2-4*a*c+4*a*A)**0.5

    term1 = dmdA*uA
    term2 = dmda*ua
    term3 = dmdb*ub
    term4 = dmdc*uc
    term5 = 2*dmda*dmdb*uab
    term6 = 2*dmda*dmdc*uac
    term7 = 2*dmdb*dmdc*ubc

    return np.sqrt(term1**2+term2**2+term3**2+term4**2+term5+term6+term7)

# Uncertainty of peka area is the standard deviation of Check Standard 4
area_uncertainty = test_pd_data.loc[test_pd_data['Sample type']=='Check standard 4', 'Fluoride Peak Area
(uS/cm*min)'].std()
print(f'Area uncertainty: {area_uncertainty}')

# open .csv file and read data
test_path = r'C:\Users\hds2\OneDrive - NIST\PREP-PFAS\CIC\CIC Liquid Injections\CIC 202504 - IF Analysis'

cals = ['Standard 1', 'Standard 2', 'Standard 5', 'Standard 10', 'Standard 20', 'Standard 50']
corresponding_vols = [200, 100, 40, 20, 10, 4] # in uL
```

```
# Fit linear and quadratic models to each anion
# Anions: Fluoride, Chloride, Bromide, Phosphate, Sulfate
for anion in ['Fluoride', 'Chloride', 'Bromide', 'Phosphate', 'Sulfate']:
    print(f'Fitting {anion} data...')
    # Get peak areas and concentrations
    peak_areas = test_pd_data[f'{anion} Peak Area (uS/cm*min)']

    # Grab only the calibration data
    cal_data = test_pd_data[test_pd_data['Sample type'].isin(cals)]
    cal_peak_areas = cal_data[f'{anion} Peak Area (uS/cm*min)']

    cal_mass = []
    # Check if there is more than one calibration solution concentration
    if len(test_cal_concs) == 1:
        # if only one calibration solution concentration, use that one
        cal_sol_conc = test_cal_concs[0]
        for sample in cal_data['Sample type']:
            if sample in cals:
                index = cals.index(sample)
                vol = corresponding_vols[index]
                mass = cal_sol_conc * vol / 1e6 # in mg
                cal_mass.append(mass)

    if len(test_cal_concs) > 1:
        # find the calibration solution concentration that matches the date and time of the test data
        for i, time in enumerate(test_cal_times):
            if time in test_pd_data['Determination start'].values:
                cal_sol_conc = test_cal_concs[i]
                for sample in cal_data['Sample type']:
                    if sample in cals:
                        index = cals.index(sample)
                        vol = corresponding_vols[index]
                        mass = cal_sol_conc * vol / 1e6 # in mg
                        cal_mass.append(mass)
```

```
    # linear fit
    lin_model = lmfit.Model(linear_fit)
    lin_params = lin_model.make_params(a=1, b=0)
    lin_result = lin_model.fit(cal_peak_areas, lin_params, m=cal_mass)

    # quadratic fit
    quad_model = lmfit.Model(quad_fit)
    quad_params = quad_model.make_params(a=0, b=1, c=0)
    quad_result = quad_model.fit(cal_peak_areas, quad_params, m=cal_mass)

    # Write fit parameters and uncertainties to a text file
    with open(folder_path + file_name + f' {anion} Fit Parameters.txt', 'w') as f:
        f.write(f'{anion} Fit Parameters and Uncertainties\n')
        f.write('----------------------------------------\n\n')
        f.write(f'Area Uncertainty: {area_uncertainty}\n\n')
        f.write('Linear Fit Parameters:\n')
        f.write(f'a: {lin_result.params["a"].value} +/- {lin_result.params["a"].stderr}\n')
        f.write(f'b: {lin_result.params["b"].value} +/- {lin_result.params["b"].stderr}\n\n')
        f.write(f'Covariance ab: {lin_result.covar[0][1]}\n\n')

        f.write('Quadratic Fit Parameters:\n')
        f.write(f'a: {quad_result.params["a"].value} +/- {quad_result.params["a"].stderr}\n')
        f.write(f'b: {quad_result.params["b"].value} +/- {quad_result.params["b"].stderr}\n')
        f.write(f'c: {quad_result.params["c"].value} +/- {quad_result.params["c"].stderr}\n')
        f.write(f'Covariance ab: {quad_result.covar[0][1]}\n')
        f.write(f'Covariance ac: {quad_result.covar[0][2]}\n')
        f.write(f'Covariance bc: {quad_result.covar[1][2]}\n')

    # Calculate masses for all samples using linear and quadratic fits
    lin_masses = linear_results(peak_areas, lin_result.params['a'].value, lin_result.params['b'].value)
    quad_masses = quad_results(peak_areas, quad_result.params['a'].value, quad_result.params['b'].value,
quad_result.params['c'].value)

    # Save masses to dataframe
    test_pd_data[f'{anion} Mass Linear (mg)'] = lin_masses
    test_pd_data[f'{anion} Mass Quadratic (mg)'] = quad_masses
```

```
    # calculate uncertainties for all samples using linear and quadratic fits
    lin_uncs = lin_fit_unc(peak_areas, lin_result.params['a'].value, lin_result.params['b'].value, area_uncertainty, lin_result.params['a'].stderr, lin_result.params['b'].stderr, lin_result.covar[0][1])
    quad_uncs = quad_fit_unc(peak_areas, quad_result.params['a'].value, quad_result.params['b'].value, quad_result.params['c'].value, area_uncertainty, quad_result.params['a'].stderr, quad_result.params['b'].stderr, quad_result.params['c'].stderr,  quad_result.covar[0][1], quad_result.covar[1][2], quad_result.covar[0][2])

    # Save uncertainties to dataframe
    test_pd_data[f'{anion} Mass Linear Unc (mg)'] = lin_uncs
    test_pd_data[f'{anion} Mass Quadratic Unc (mg)'] = quad_uncs

test_pd_data.to_csv(folder_path + file_name + ' fits.csv', index=False)
```

C.2. Organofluorine and Organochlorine Calibration Curve

```
import pandas as pd
import lmfit
import os
linear_model = lmfit.Model(lambda x, m, b: m*x + b)
quadratic_model = lmfit.Model(lambda x, a, b, c: a*x**2 + b*x + c)
fluorine_data = pd.read_excel('fluorine_curves.xlsx')
names = ['RM8446PtA', 'RM8446PtB', 'SRM21432144', 'SRM3183', 'SRM3182', 'SRM3184']
anions=['F', 'Cl', 'Br']
f_data = fluorine_data[fluorine_data['Element'] == 'F']
f_types = ["RM8446PtA", "RM8446PtB", "SRM21432144", "DINJF", "SRM3183"]
out_file = 'fluorine_curve_fits.xlsx'
fit_params = []

for ft in f_types:
    subset = f_data[f_data['Name'] == ft]
    x = subset['InjMass (ng)']
    y = subset['PeakArea']
    x_unc = subset['InjMassUnc(ng)']
    y_unc = subset['AreaUnc']
```

```
    linear_params = linear_model.make_params(m=1, b=0)
    linear_fit = linear_model.fit(y, linear_params, x=x)
    quadratic_params = quadratic_model.make_params(a=0, b=1, c=0)
    quadratic_fit = quadratic_model.fit(y, quadratic_params, x=x)

    # write to excel (use 'w' when file doesn't exist, 'a' otherwise)
    mode = 'a' if os.path.exists(out_file) else 'w'
    with pd.ExcelWriter(out_file, mode=mode, engine='openpyxl', if_sheet_exists='replace') as writer:
        fit_df = pd.DataFrame({
            'InjMass (ng)': x,
            'PeakArea': y,
            'AreaUnc': y_unc,
            'InjMassUnc(ng)': x_unc,
            'Linear_Fit': linear_fit.best_fit,
            'Quadratic_Fit': quadratic_fit.best_fit
        })
        fit_df.to_excel(writer, sheet_name=ft, index=False)

        # Also write fit parameters
        params_df = pd.DataFrame({
            'Parameter': list(linear_fit.params.keys()) + list(quadratic_fit.params.keys()),
            'Linear_Value': [linear_fit.params[p].value for p in linear_fit.params] + [None]*len(quadratic_fit.params),
            'Linear_Stderr': [linear_fit.params[p].stderr for p in linear_fit.params] + [None]*len(quadratic_fit.params),
            'Quadratic_Value': [None]*len(linear_fit.params) + [quadratic_fit.params[p].value for p in
quadratic_fit.params],
            'Quadratic_Stderr': [None]*len(linear_fit.params) + [quadratic_fit.params[p].stderr for p in
quadratic_fit.params],
        })
        params_df.to_excel(writer, sheet_name=ft+'_Params', index=False)

    # append fits to list
    fit_params.append({
        'Name': ft,
        'Linear_Fit': linear_fit,
        'Quadratic_Fit': quadratic_fit
    })
```

```
# Chlorine
cl_data = fluorine_data[fluorine_data['Element'] == 'Cl']
cl_types = ["SRM21432144", "DINJCl", "SRM3182"]
cl_fit_params = []

for ct in cl_types:
    subset = cl_data[cl_data['Name'] == ct]
    x = subset['InjMass (ng)']
    y = subset['PeakArea']
    x_unc = subset['InjMassUnc(ng)']
    y_unc = subset['AreaUnc']

    linear_params = linear_model.make_params(m=1, b=0)
    linear_fit = linear_model.fit(y, linear_params, x=x)
    quadratic_params = quadratic_model.make_params(a=0, b=1, c=0)
    quadratic_fit = quadratic_model.fit(y, quadratic_params, x=x)

    # write to excel (use 'w' when file doesn't exist, 'a' otherwise)
    mode = 'a' if os.path.exists(out_file) else 'w'
    with pd.ExcelWriter(out_file, mode=mode, engine='openpyxl', if_sheet_exists='replace') as writer:
        fit_df = pd.DataFrame({
            'InjMass (ng)': x,
            'PeakArea': y,
            'AreaUnc': y_unc,
            'InjMassUnc(ng)': x_unc,
            'Linear_Fit': linear_fit.best_fit,
            'Quadratic_Fit': quadratic_fit.best_fit
        })
        fit_df.to_excel(writer, sheet_name=ct, index=False)

        # Also write fit parameters
        params_df = pd.DataFrame({
            'Parameter': list(linear_fit.params.keys()) + list(quadratic_fit.params.keys()),
            'Linear_Value': [linear_fit.params[p].value for p in linear_fit.params] + [None]*len(quadratic_fit.params),
            'Linear_Stderr': [linear_fit.params[p].stderr for p in linear_fit.params] + [None]*len(quadratic_fit.params),
```

```
        'Quadratic_Value': [None]*len(linear_fit.params) + [quadratic_fit.params[p].value for p in
quadratic_fit.params],
        'Quadratic_Stderr': [None]*len(linear_fit.params) + [quadratic_fit.params[p].stderr for p in
quadratic_fit.params],
      })
      params_df.to_excel(writer, sheet_name=ct+'_Params', index=False)


   # append fits to list
   cl_fit_params.append({
      'Name': ct,
      'Linear_Fit': linear_fit,
      'Quadratic_Fit': quadratic_fit
   })
# bromine
br_data = fluorine_data[fluorine_data['Element'] == 'Br']
br_types = ["DINJBr", "SRM3184"]
br_fit_params = []

for bt in br_types:
   subset = br_data[br_data['Name'] == bt]
   x = subset['InjMass (ng)']
   y = subset['PeakArea']
   x_unc = subset['InjMassUnc(ng)']
   y_unc = subset['AreaUnc']

   linear_params = linear_model.make_params(m=1, b=0)
   linear_fit = linear_model.fit(y, linear_params, x=x)
   quadratic_params = quadratic_model.make_params(a=0, b=1, c=0)
   quadratic_fit = quadratic_model.fit(y, quadratic_params, x=x)

   # write to excel (use 'w' when file doesn't exist, 'a' otherwise)
   mode = 'a' if os.path.exists(out_file) else 'w'
   with pd.ExcelWriter(out_file, mode=mode, engine='openpyxl', if_sheet_exists='replace') as writer:
      fit_df = pd.DataFrame({
         'InjMass (ng)': x,
         'PeakArea': y,
```

```
            'AreaUnc': y_unc,
            'InjMassUnc(ng)': x_unc,
            'Linear_Fit': linear_fit.best_fit,
            'Quadratic_Fit': quadratic_fit.best_fit
        })
        fit_df.to_excel(writer, sheet_name=bt, index=False)

        # Also write fit parameters
        params_df = pd.DataFrame({
            'Parameter': list(linear_fit.params.keys()) + list(quadratic_fit.params.keys()),
            'Linear_Value': [linear_fit.params[p].value for p in linear_fit.params] + [None]*len(quadratic_fit.params),
            'Linear_Stderr': [linear_fit.params[p].stderr for p in linear_fit.params] + [None]*len(quadratic_fit.params),
            'Quadratic_Value': [None]*len(linear_fit.params) + [quadratic_fit.params[p].value for p in
quadratic_fit.params],
            'Quadratic_Stderr': [None]*len(linear_fit.params) + [quadratic_fit.params[p].stderr for p in
quadratic_fit.params],
        })
        params_df.to_excel(writer, sheet_name=bt+'_Params', index=False)

    # append fits to list
    br_fit_params.append({
        'Name': bt,
        'Linear_Fit': linear_fit,
        'Quadratic_Fit': quadratic_fit
    })
```

Appendix D. Additional Data and Figures

D.1. Sensitivity Figures

Circles represent outliers, lines within the boxes represent the median, boxes represent the first to third quartile of the data, and whiskers represent the farthest data point lying within the 1.5x the inter-quartile range. Outliers are defined as any data points that fall outside of the 1.5x the inter-quartile range.

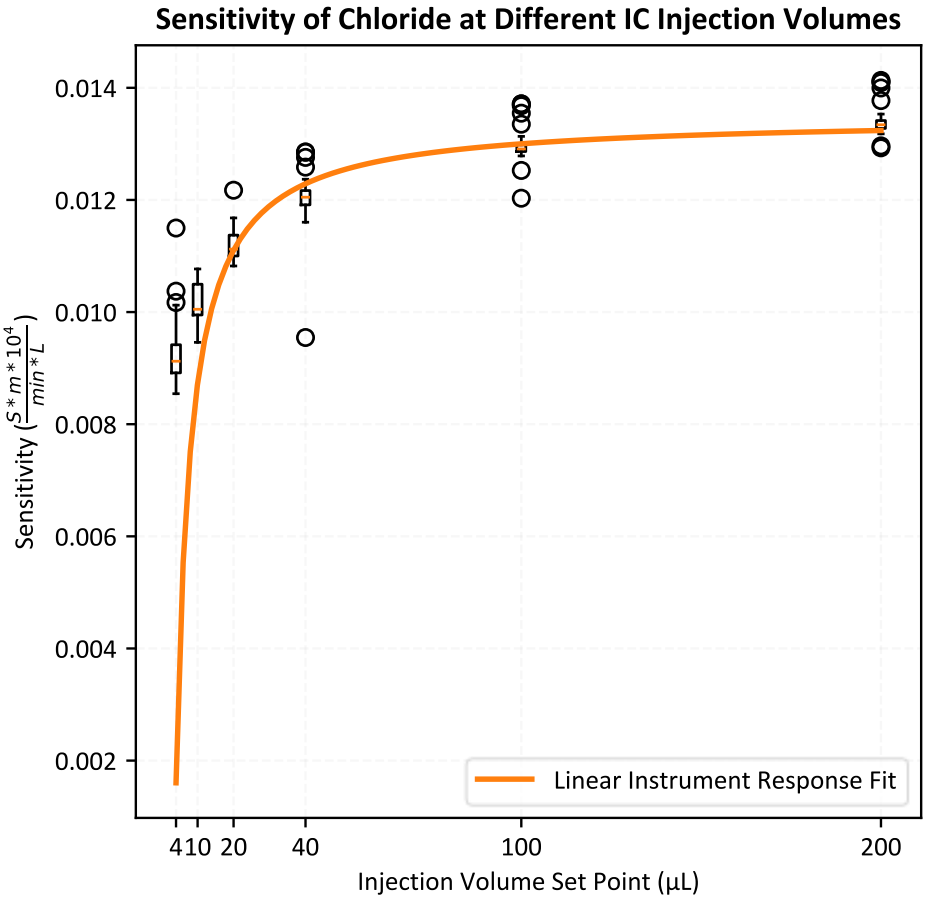

Figure 15. Sensitivity of chloride and corresponding linear instrument response fit.

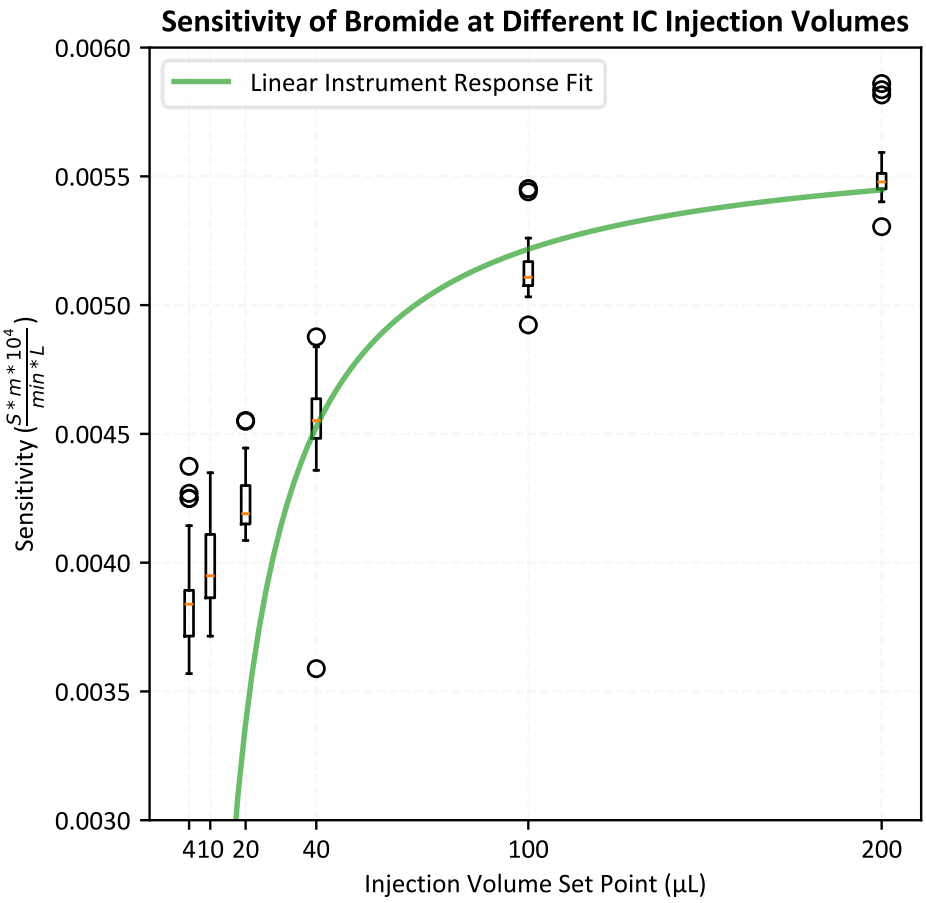

Figure 16. Sensitivity of bromide and corresponding linear instrument response fit.

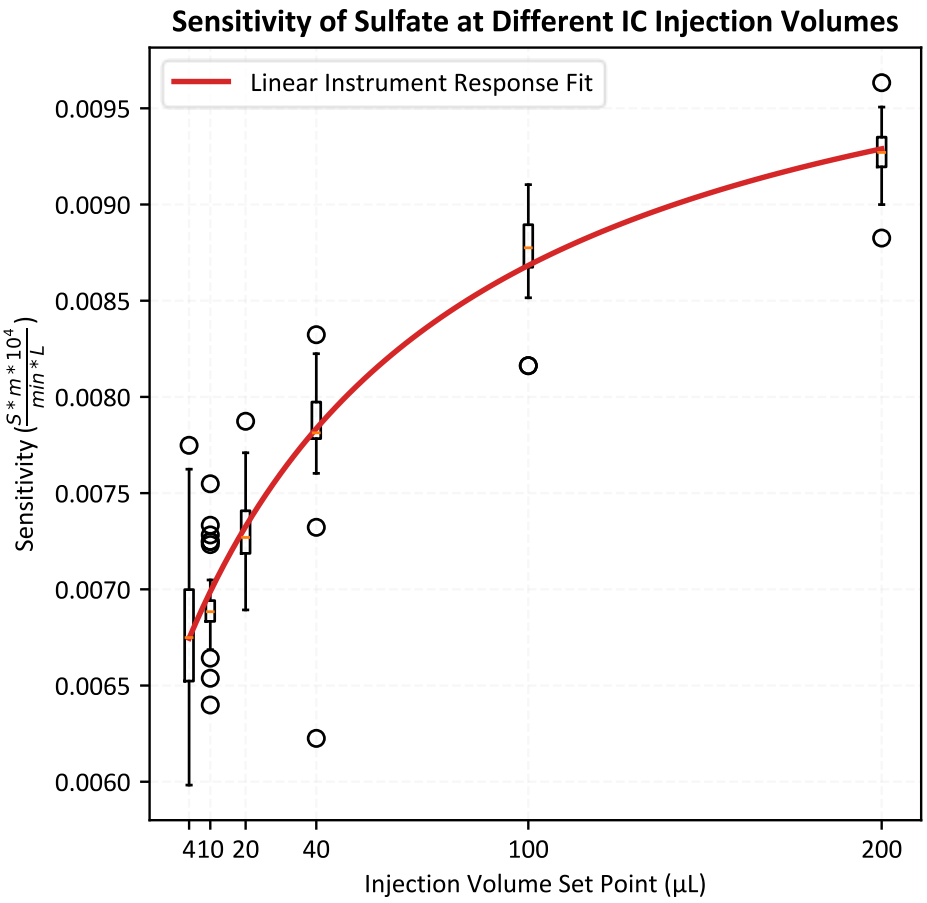

Figure 17. Sensitivity of sulfate and corresponding linear instrument response fit.

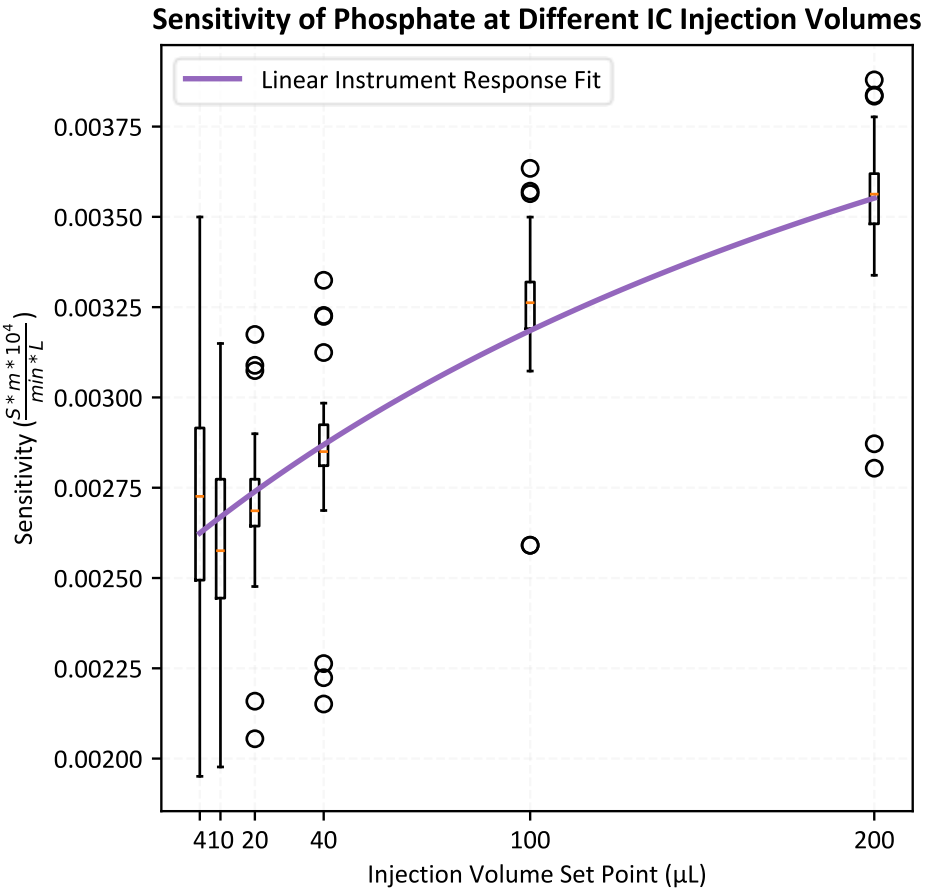

Figure 18. Sensitivity of phosphate and corresponding linear instrument response fit.

D.2. Output from Calibration Curve Fits

Table 60. Fitting results from RM 8446 Part A.

Parameter	Linear_Value	Linear_Stderr	Quadratic_Value	Quadratic_Stderr
m	0.023219738	0.000301332		
b	0.014373443	0.027860365		
a			-7.44346E-06	5.95245E-06
b			0.024709514	0.001227617
c			-0.014556065	0.035846807

Table 61. Fitting results from RM 8446 Part B.

Parameter	Linear_Value	Linear_Stderr	Quadratic_Value	Quadratic_Stderr
m	0.020201089	0.000296049		
b	-0.031935335	0.031925743		
a			6.19841E-06	5.02378E-06
b			0.01876191	0.001202279
c			0.001886693	0.041695139

Table 62. Fluoride fitting results from SRM 2143/2144.

Parameter	Linear_Value	Linear_Stderr	Quadratic_Value	Quadratic_Stderr
m	0.017592	0.000142		
b	0.060119	0.024457		
a			-4E-06	1.01E-06
b			0.019179	0.000415
c			-0.00855	0.025285

Table 63. Chloride fitting results from SRM 2143/2144.

Parameter	Linear_Value	Linear_Stderr	Quadratic_Value	Quadratic_Stderr
m	0.012258558	0.000122723		
b	-0.029110721	0.02147951		
a			3.12475E-06	9.16519E-07
b			0.010997889	0.000382605
c			0.026293937	0.023664244

Table 64. Fluoride fitting results from direct injections.

Parameter	Linear_Value	Linear_Stderr	Quadratic_Value	Quadratic_Stderr
m	0.016509991	0.000346457		
b	0.139529059	0.066322353		
a			-1.29106E-05	9.17395E-07
b			0.021879938	0.000393211
c			-0.077176263	0.02382126

Table 65. Fluoride fitting results from SRM 3183.

Parameter	Linear_Value	Linear_Stderr	Quadratic_Value	Quadratic_Stderr
m	0.017992434	0.00018503		
b	0.048940893	0.02778291		
a			-7.78154E-06	1.02621E-06
b			0.020659915	0.00036382
c			-0.035778357	0.017862756

Table 66. Chloride fitting results from direct injections.

Parameter	Linear_Value	Linear_Stderr	Quadratic_Value	Quadratic_Stderr
m	0.013428952	8.29652E-05		
b	-0.086016613	0.015882028		
a			2.80597E-06	4.00734E-07
b			0.012261854	0.000171761
c			-0.038918119	0.010405535

Table 67. Chloride fitting results from SRM 3182.

Parameter	Linear_Value	Linear_Stderr	Quadratic_Value	Quadratic_Stderr
m	0.011385695	4.62761E-05		
b	-0.038131946	0.006980734		
a			5.12136E-07	5.09093E-07
b			0.011209323	0.000181325
c			-0.032504381	0.008943943

Table 68. Bromide fitting results from direct injections.

Parameter	Linear_Value	Linear_Stderr	Quadratic_Value	Quadratic_Stderr
m	0.005508769	6.17734E-05		
b	-0.056096397	0.011825284		
a			2.30608E-06	1.59646E-07
b			0.004549589	6.84272E-05
c			-0.017388493	0.004145413

Table 69. Bromide fitting results from SRM 3184.

Parameter	Linear_Value	Linear_Stderr	Quadratic_Value	Quadratic_Stderr
m	0.004600065	3.77254E-05		
b	-0.025363027	0.005687438		
a			1.43263E-06	2.61007E-07
b			0.004106985	9.29077E-05
c			-0.009639632	0.004579959

D.3. Example Chromatograph of NIST SRM Anions

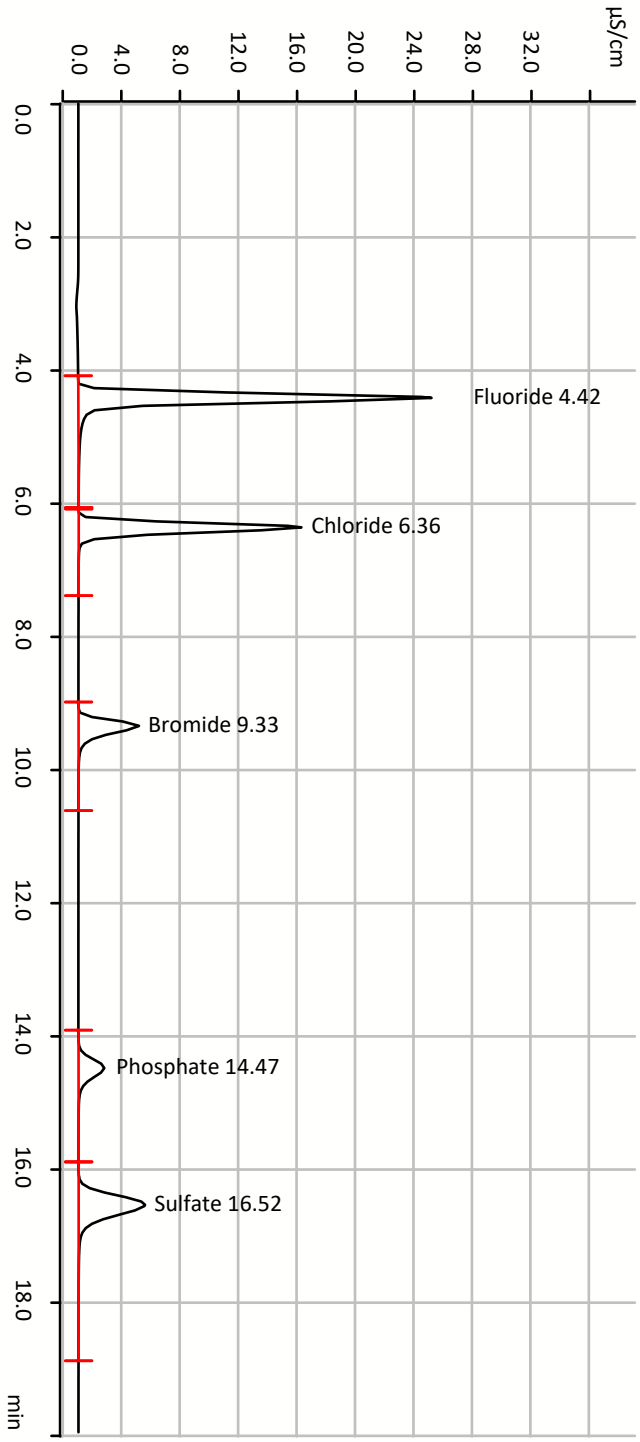

Figure 19. Example chromatograph of a solution containing 1 mg/kg each of NIST SRM 3183 (Fluoride), 3182 (Chloride), 3184 (Bromide), 3186 (Phosphate), and 3181 (Sulfate). Retention times are listed in minutes.

D.4. Example Chromatograph of 3rd Party ISO-Certified and NIST-Traceable Anion Solution (ERA Custom Mix 3)

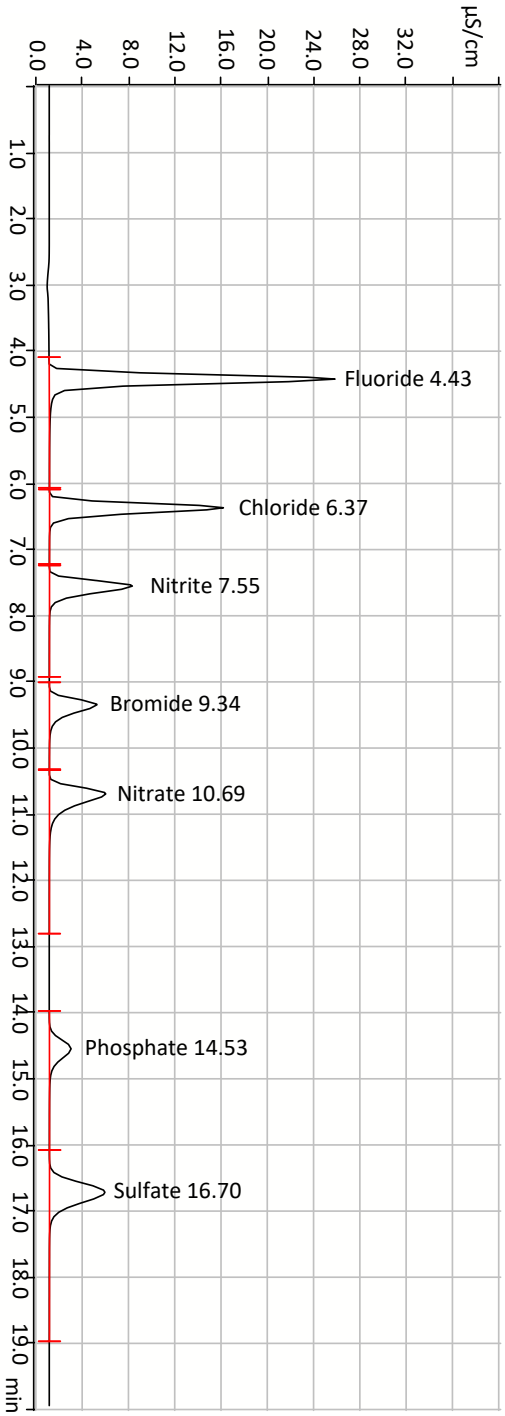

Figure 20. Example chromatograph of anion solution (ERA Custom Mix 3) containing fluoride, chloride, nitrite, bromide, nitrate, phosphate, and sulfate.

Appendix E. Effects of Glassware on Fluoride Measurements

HPLC-grade methanol was aliquoted using a pipette with a polyethylene tip into triplicates of either 1) 2 mL HPLC vials as is, 2) 2 mL HPLC vials with 250 µL glass inserts as is, 3) 2 mL HPLC vials washed using the protocols mentioned in this TN, or 4) 2 mL HPLC vials with 250 µL glass inserts washed. The vials were let to incubate for 24 hours at 20 °C. After, approximately 79.19 mg of the resulting solution was combusted with an IC injection volume of 200 µL. **Table 70** lists the values.

The values reported here should be only used as a reference, as HPLC vials and glass inserts from various lots were interchangeably used.

Table 70. Methanol blank values.

Vial Type	Amount of Methanol Aliquoted (µL)	Apparent Fluoride Mass Fraction (mg/kg)
2 mL HPLC vials as-is.	1000	4.31
2 mL HPLC with glass insert as-is.	200	1.50
2 mL HPLC vials washed.	1000	0.934
2 mL HPLC vials with washed glass insert.	200	<LOD

Appendix F. List of Symbols, Abbreviations, and Acronyms

TN
Technical Note

SRM
Standard Reference Material

RM
Reference material

PFAS
Per- and poly-fluorinated alkyl substances

PCB
Polychlorinated biphenyls

PBDE
Polybrominated diphenyl ethers

IC
Ion Chromatography

CIC
Combustion Ion Chromatography

HPLC
High-performance liquid chromatography

UPW
Ultra-pure water

SNR
Signal-to-noise ratio

4:2 FTOH
2-Perfluorobutyl ethanol [CAS: 2043-47-2]

5:2 sFTOH
1-Perfluoropenthyl ethanol (5:2 secondary) [CAS: 914637-05-1]

8:2 FTOH
2-Perfluorooctyl ethanol [CAS: 678-39-7]

10:2 FTOH
2-Perfluorodecyl ethanol [CAS: 865-86-1]

8:2 FTAcr
1H, 1H, 2H, 2H-Perlfuorodecyl acrylate [CAS: 27905-45-9]

PFHxA
Perfluorohexanoic acid [CAS: 307-24-4]

PFHpA
Perfluoroheptanoic acid [CAS: 375-85-9]

PFOA

Perfluorooctanoic acid [CAS: 335-67-1]

PFNA
Perfluorononanoic acid [CAS: 375-95-1]

PFDA
Perfluorodecanoic acid [CAS: 335-76-2]

PFUnA
Perfluoroundecanoic acid [CAS: 2058-94-8]

PFDoA
Perfluorododecanoic acid [CAS: 307-55-1]

PFTriA
Perfluorotridecanoic acid [CAS: 72629-94-8]

PFTA
Perfluorotetradecanoic acid [CAS: 376-06-7]

PFBA
Perfluorobutanoic acid [CAS: 375-22-4]

PFPeA
Perfluoropentanoic acid [CAS: 2706-90-3]

PFOSA
Perfluorooctane sulfonamide [CAS: 754-91-6]

CCV
Calibration curve validity

RSD
Relative standard deviation

STP
Standard Temperature and Pressure